Ozonation using hollow fiber contactor technology and its perspectives for micropollutants removal in water: A review

Alice Schmitt, Julie Mendret, Michel Roustan, S. Brosillon

Ozonation using hollow fiber contactor technology and its perspectives for micropollutants removal in water: a review

Alice Schmitt[a], Julie Mendret[a], Michel Roustan[b], Stephan Brosillon[a]

[a] IEM (Institut Européen des Membranes), UMR 5635 (CNRS-ENSCM-UM2), Université Montpellier 2, Place E. Bataillon, F-34095 Montpellier, France

[b] TBI, Université de Toulouse, CNRS, INRA, INSA, Toulouse, France

Submitted to Science of the Total Environment

Corresponding author:

Julie Mendret

IEM (Institut Européen des Membranes), UMR 5635 (CNRS-ENSCM-UM2),

Université Montpellier 2, Place E. Bataillon, F-34095 Montpellier, France

Tel: +33 467144624 ; Fax: +33 467149119

E-mail: julie.mendret@umontpellier.fr

Abstract

Membrane contactor is a device generally used for the removal or the absorption of a gas into another fluid. The membrane acts as a barrier between the two phases and mass transfer occurs by diffusion and not by dispersion. This article is a review of the application of membrane contactor technology for ozonation applied to water treatment. The challenge of removing micropollutants is also discussed. In the first part, the ozonation process is mentioned, in particular chemical reactions induced by ozone and its advantages and disadvantages. In the second part, generalities on membrane contactor technology using hollow fibers are presented. Then, the benefit of using a membrane contactor for the elimination of micropollutants is shown through a critical analysis of the influence of several parameters on the ozonation efficiency. The impact of the membrane material is also highlighted. Finally, several modeling approaches are presented as a tool for a better understanding of the phenomena occurring in the contactor and a possible optimization of this process.

Keywords: Membrane contactor; Ozonation; Micropollutants; Mass transfer; Modeling

1. Introduction

To protect the ecosystem and drinking water resources, requirements on water treatment will become increasingly stricter. It is only a matter of time before treatment plants will be required to incorporate treatment steps to ensure that micropollutants (i.e. harmful substances, detectable in the environment at very low concentrations (ng/L up to µg/L)) are eliminated and do not enter the water bodies. For instance, in Switzerland, a new Swiss water protection act entered into force in 2016 aiming to reduce the discharge of micropollutants from wastewater treatment plants (WWTPs) (Office fédéral de l'environnement, 2014). As a consequence, selected WWTPs must be upgraded by an advanced treatment for micropollutants abatement with suitable and economic options such as ozonation. Ozone treatment is easy to automate and clean to handle. It provides a chemical-free means of removing 90 percent of emerging contaminants (Prieto-Rodríguez et al., 2013; Snyder et al., 2006). It can be quite simply incorporated into existing and new applications and is a reliable and control-supported process. Another advantage of ozonation is the direct oxidation, breaking the molecule which is destroyed and not only absorbed. Ozonation is thus an interesting technology for water reuse since it can both disinfect and oxidize, or be used with other technologies in a multiple-barrier concept.

The conventional reactors used during the ozonation processes are presented in Table 1. A schematic drawing of each reactor is exposed in Figure 1. Depending on the application (i.e. the objectives of the ozonation), the reactor is chosen according to its contact time (especially for slow reactions), its hydrodynamics (especially for fast and moderately fast reaction, where a plug flow is preferable), and its ozone transfer (especially for very fast reaction, where a high interfacial area is preferable). Generally, ozone in water treatment is injected in the form

66 of bubbles, with disadvantages such as operational costs, stripping of volatile organic
67 compounds, high footprint of the reactor, mass transfer limitations (leading to high energetic
68 costs) and foam generation. Moreover, in some cases, these processes do not ensure a
69 controlled dosage, and can lead to the production of by-products sometimes more dangerous
70 than the original products (Gao et al., 2016; Gogoi et al., 2018; Schlüter-Vorberg et al., 2015).

71

72 Table 1: Conventional reactors used for ozonation, adapted from Suez, 2007

Type of reactor	Dispersed phase	Value range of kLa according to the literature (s-1)	Value range of gas retention Ɛg	Value range of power consumption (kW.m-3 of reactor)	Advantages	Disadvantages	Application fields
Bubble column with porous diffusers	Gas	0.0001-0.1 (K_La between 0.005 and 0.12 (Chabanon and Favre, 2017))	< 0,2	0.01- 1	Smooth operation Low maintenance cost	Risk of clogging Complex hydrodynamics	Drinking water (Low ozone dose transferred and slow reaction)
Turbine engine or with radial diffuser	Gas	0.01-0.2	< 0.1	0.5 - 4	Gas/Liquid mix and contact Flexible to the variation in the liquid flow	High energy consumption Mechanical equipment maintenance	Drinking water and wastewater (High ozone dose transferred, moderately fast reaction)
Packed column	Liquid	0.005-0.02 K_La between 0.0004 and 0.07 (Chabanon and Favre, 2017))	> 0.3	0.01 - 0.2	Transfer and plug flow Low maintenance cost	Risk of fouling of the lining	Gas washing, production of ozonated water (Fast reaction)
Static mixer	Gas	0.1-10	Around 0.5	10 - 200	Mix and transfer Low maintenance cost Low size of installation	High energy consumption Short contact time Risk of clogging	Drinking water and wastewater (Very fast reaction)

Venturi injector	Gas	0.06-0.21 (Roustan, 2003)	1-10 (Roustan, 2003)	N.A.	High mass transfer (Cachon et al., 2019; Ozkan et al., 2006) High gas-liquid interfacial area High energy efficiency Applicable to short contact time (Briens et al., 1992) No additional equipment needed (i.e. located directly in the process stream) (Bauer et al., 1963) Minimal maintenance (Cachon et al., 2019)	Power from a recirculating pump required, or pressurized water supply (Cachon et al., 2019)	Petroleum refining, Hydrogenation, Fermentation, Waste-water treatment (Briens et al., 1992)

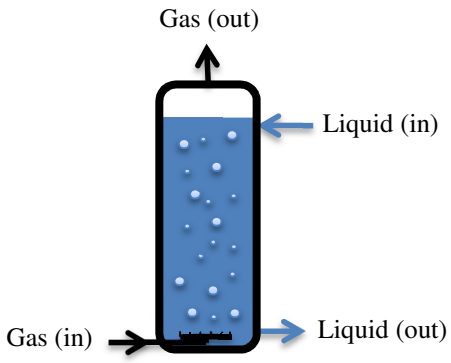

Bubble column

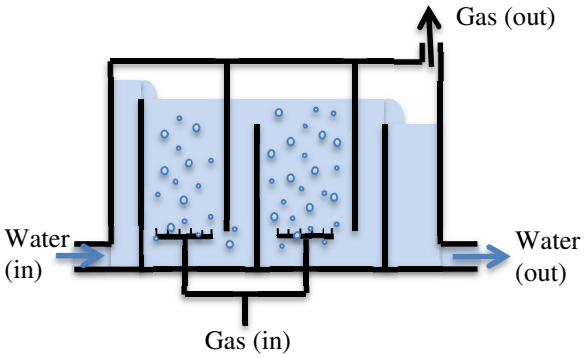

Ozonation reactor with multiple chambers

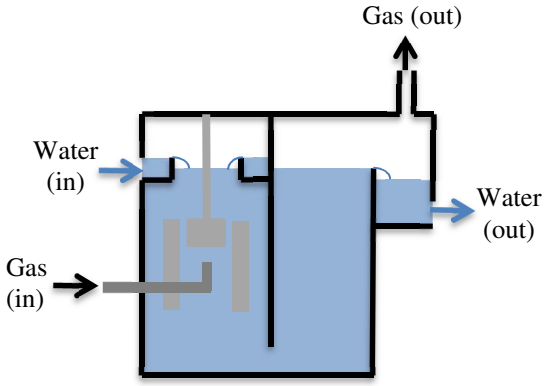

Turbine engine

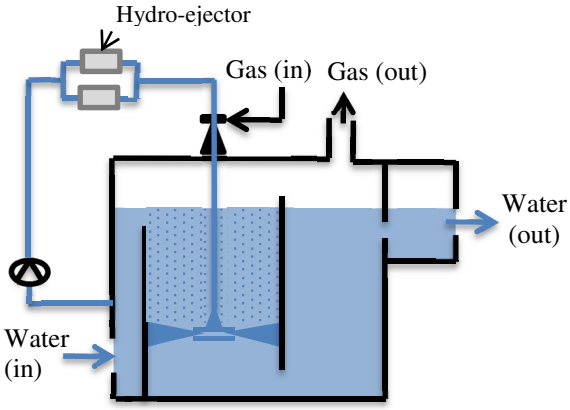

Reactor with radial diffusor

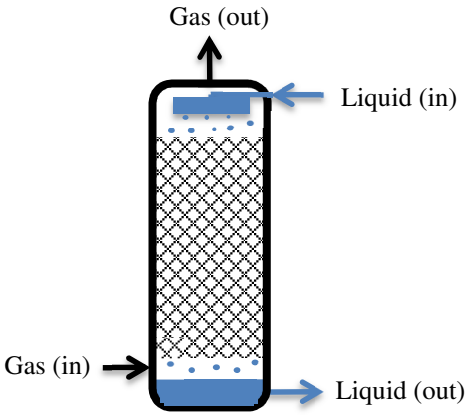

Packed column

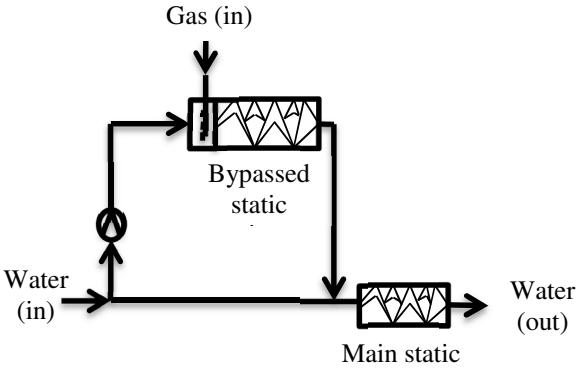

Static mixer system

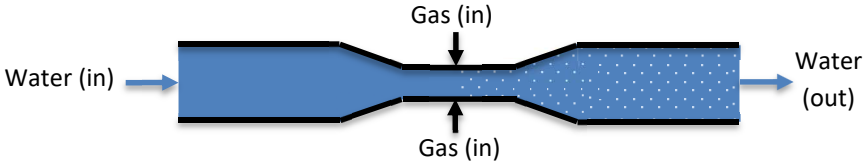

Venturi injector

77 Figure 1: Schemes of conventional reactors used for ozonation

78 The use of membrane contactors for ozone diffusion in water treatment recently emerged as a
79 very interesting option. Indeed, by using a bubbleless operation, membrane contactors can
80 overcome these challenges. Indeed, membrane contactors have been pointed out as a good
81 alternative for the transfer of gas to the liquid phase (Alves dos Santos et al., 2015; Berry et
82 al., 2017; Pabby and Sastre, 2013; Stylianou et al., 2016), and to control the dosage of ozone
83 during ozonation processes (Atchariyawut et al., 2009; Bamperng et al., 2010; Berry et al.,
84 2017; Janknecht et al., 2001; Jansen et al., 2005; Leiknes et al., 2005; Merle et al., 2017;
85 Picard et al., 2001; Pines et al., 2005; Shanbhag et al., 1998, 1995; Stylianou et al., 2018,
86 2016; Wenten et al., 2012; Zoumpouli et al., 2018). The following list describes the major
87 advantages of a membrane contactor technology:

88 • This process has a smaller foot print than conventional reactor, thanks to its large
89 interfacial area. Since treatment of wastewater are targeted, very fast reaction will
90 occur and thus the transfer will be accelerated by the reaction, as a consequence it is
91 interesting to develop high interfacial area in the reactors. According to Reed et al.,
92 membrane contactors have an interfacial area between 1640 and 6562 m^2/m^3.
93 According to Chabanon et al., membrane contactors have a surface area/volume ratio
94 around 1,000-10,000 m²/m3, whereas this ratio is between 50 and 600 m²/m3 for a
95 bubble column and between 10 and 500 m²/m3 for a packed column. (Chabanon and
96 Favre, 2017). In contrast, conventional contactors have an interfacial area between 3
97 and 492 m^2/m^3.(Reed et al., 1995). Pines et al (2005) have carried out calculations, an
98 hypothetical case of 167 m^3/h flow rate and 2 mg/L transferred ozone dose was used in
99 order to compare the volume required for hollow fiber membrane contactors (PVDF)
100 configurations compared to a fine-bubble diffuser contactor. The assumptions were a
101 gas O_3 concentration of about 6%, no chemical reaction and a system mass transfer
102 limited. Stylianou et al (2016) have carried out the same calculations based on their

experimental results obtained with ceramic tubular membrane. The volume of each reactor was 12 m^3, 1.9 m^3 and 0.15 m^3 respectively for bubble column; ceramic tubular membrane contactor and PVDF hollow fiber membrane. This first approach demonstrates the real interest of membrane contactor to increase the compactness of the unit operation.

- The mass transfer (i.e. the KLa) obtained with a membrane contactor is significantly higher than with other conventional reactors. For a membrane contactor, the mass transfer is estimated between 0.05 and 0.50 s-1, whereas it is between 0.005 and 0.12 s-1 for a bubble column and between 0.0004 and 0.07 s-1 for a packed column. The difference is mainly due to a surface area/volume ratio particularly interesting with the membranes.
- The compound of interest (i.e. here the ozone molecule) has a uniform distribution, thanks to the large exchange surface (i.e. interfacial area) offered by the hollow fiber membranes.
- The risk of flooding and of entrainment of the dispersed phase is avoided thanks to a bubbleless process.
- Increasing the production capacity of a membrane contactor is easy by adding more membrane modules (i.e. this process is especially modular).
- The exchange surface is independent of the flow rates. The process can work efficiently at different gas/liquid ratios, and therefore has a wide range of capacities for the same number of modules.
- Operations are performed under low pressures because transfer is driven by the concentration gradient and not by the pressure gradient. Therefore, energy requirement by this process is lower.

- A gas stream recycling can be implemented, and thus energy and reagent savings can be made.
- Thanks to the independent flow adjustment for gas and liquid phases, an optimization of applied reagent dosage (i.e. here ozone) also allows to save reagent.
- All the ozone diffused through the membrane is transferred into the liquid phase (reacting or not in this phase), due to the bubbleless process. The rest (in the gas phase) can be recycled to the ozone generator thanks to a lower moisture content than in conventional processes (Phattaranawik et al., 2005; Stylianou et al., 2016). In comparison to bubble column where 25% of ozone is not transferred in the liquid phase, fewer reagents are needed for the same oxidation.
- Less by-products (e.g. bromates) could be produced than in conventional ozonation processes thanks to the minimization of the dissolved ozone concentration ((Heeb et al., 2014; Merle et al., 2017).

On the contrary, according to several studies, the main disadvantages of the membrane contactor process are the following (Gabelman and Hwang, 1999; Mulder, 1996).

- The risk of wetting is important and depends on the transmembrane pressure. Its consequence is a lower ozone transfer.
- A risk of bubbling is common and also depends on the transmembrane pressure. Ozone which is diffused by bubbles through the membrane may not be completely transferred into the liquid phase, and thus stays in gaseous form.
- The liquid can cause the fouling of the fibers. Fouling is one of the main problems in the application of porous membrane for water treatment (Van Geluwe et al., 2011). Gas/liquid contactors are less sensitive to fouling than filtration membranes) because no flow circulates through the membrane pores (Van Geluwe et al., 2011; Yu et al.,

151 2015). However, membrane contactors have generally a small diameter, and therefore
152 suspended particles in the gas phase or in the liquid phase can cause plugging (Van
153 Geluwe et al., 2011). When the gas circulates in the lumen and the liquid in the shell
154 side, this phenomenon is limited. There is little available literature on ozone transfer
155 into water with membranes, and to date no literature concerning the fouling during
156 such a process. Most studies focus on ozone as a pretreatment (i.e. as a supplementary
157 agent) within hybrid treatment processes, leading to the reduction of fouling or the
158 increase of the biodegradation of contaminants in membrane bioreactor, and therefore
159 to better membrane performances (Kim et al., 2008; Laera et al., 2012; Van Geluwe et
160 al., 2011; Zoumpouli et al., 2018).

161 • The overall resistance to transfer is increased due to the addition of a new phase (i.e.
162 the membrane).

163 • A bypass may be created into the shell side. If the liquid is in the shell side, a part of
164 the water could not be treated. If the gas is in the shell side, a part of the oxidizing
165 compound could not be transferred in the other phase.

166 In recent years, very interesting reviews on advanced oxidation processes for water treatment
167 were generated, but none concerning the ozonation with membrane contactors (Von Gunten,
168 2018). In this context, this review focuses on the ozonation of water using membrane
169 contactors, that had not yet been previously reviewed in detail. Hollow fibers and tubular
170 technologies for the elimination of micropollutants in water are described more specifically.
171 The significance of the membrane material is highlighted, as well as the importance of the
172 modeling in order to optimize the transfer. Conversely, processes like ozonation on catalytic
173 membranes, or ozonation for cleaning, are not covered.

174

2. General principles of ozonation

2.1. Ozonation reaction

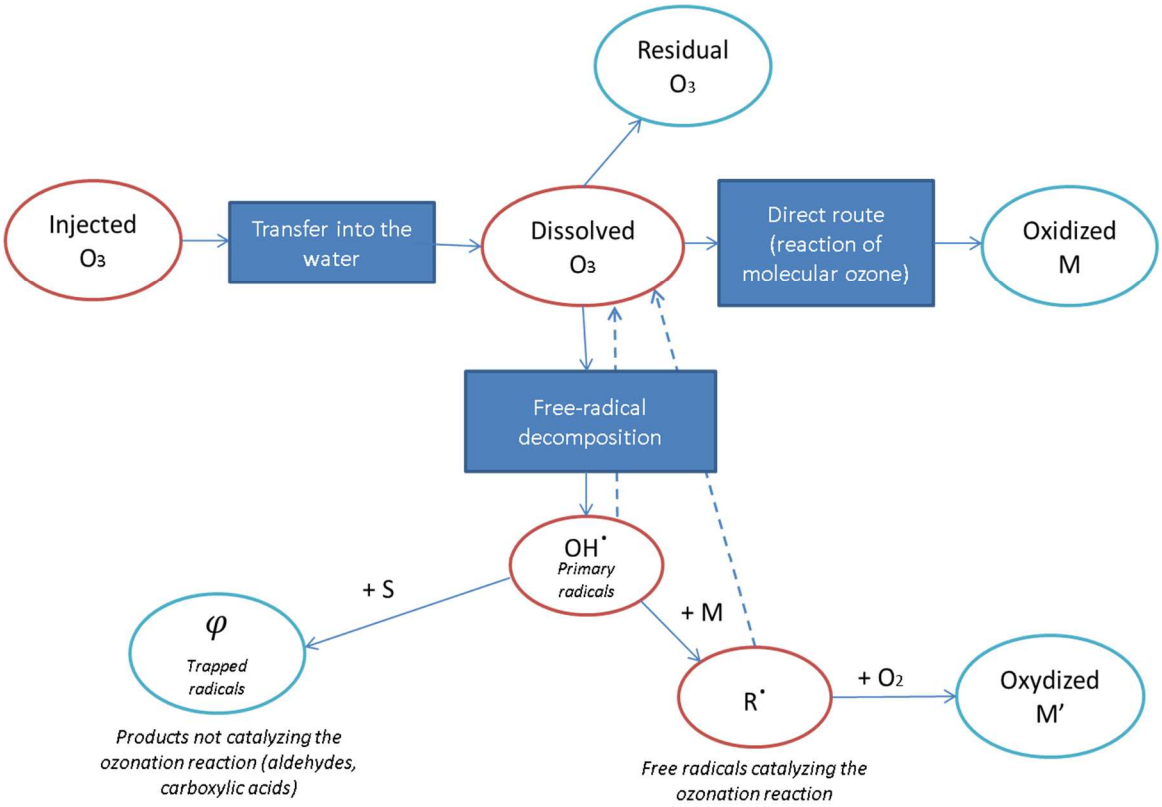

Figure 2: Ozonation reaction in water during oxidation of a pollutant M

The ozonation reaction is described in Figure 2 (Nawrocki and Kasprzyk-Hordern, 2010). Several mechanisms occur simultaneously and by chain reactions during degradation of an organic substance M. In the first case, molecular ozone can directly oxidize the polluting substance. In the second case, ozone can decompose into hydroxyl radicals. This way leads to a succession of radical reactions, initiated by the interaction between hydroxyl radicals and ozone (Gordon, 1995; Westerhoff et al., 1997). Hydroxyl radicals are non-selective and have strong oxidation properties (Kanakaraju et al., 2018).

These mechanisms coexist and the kinetic expression of the reaction can be described by equation 1:

$$r_M = k_{O3}[O_3][M] + k_{OH}[OH^\circ][M]$$

$$= [O_3][M][k_{O3} + k_{OH}R] \quad [1]$$

Where:

- r_M: reaction rate ($mol.L^{-1}.s^{-1}$)
- [HO°]: concentration of hydroxyl radicals ($mol.L^{-1}$)
- $[O_3]$: concentration of molecular ozone ($mol.L^{-1}$)
- k_{O3} , k_{HO°: second-order rate constant for the reaction of micropollutant (M) with O_3 and HO° ($L.\ mol^{-1}s^{-1}$)
- R=[HO°]/$[O_3]$: ratio between the concentration of hydroxyl radicals and the concentration of molecular ozone, varying between 10^{-9} and 10^{-7} and depending on the water type (according to Elovitz et al., 2000)

The mechanism favoring the oxidation efficiency depends on the k_{O3} value, which is a second order rate constant. When $k_{O3} < 100\ mol.L^{-1}.s^{-1}$, the main way of degradation is the radical mechanisms. When k_{O3} is between 100 and 10,000 $mol.L^{-1}.s^{-1}$, both radical and molecular mechanisms occur simultaneously with the same order of magnitude. When $k_{O3} > 10{,}000\ mol.L^{-1}.s^{-1}$, molecular mechanisms are promoted. (Bourgin et al., 2017)

2.1. Ozonation efficiency for the elimination of micropollutants in water

Advanced treatment technologies remove MP more efficiently than primary and secondary treatments (Luo et al., 2014). Several studies about the application of ozonation for MP elimination have been carried out (Behera et al., 2011; Huber et al., 2003; Lishman et al., 2006; Paxéus, 2004; Santos et al., 2007). Ozone eliminates a wide range of MP in WWTP, with a dose of dissolved ozone around 3-8 mgO_3/L (Gomes et al., 2017; Hollender et al.,

2009; Margot et al., 2013; Nakada et al., 2007; Reungoat et al., 2012, 2010; Rosal et al., 2010). This process is also efficient on several pharmaceuticals often detected in surface waters (Tootchi et al., 2013). The degradation efficiency of MP depends on several parameters (see 2.3. Influential parameters), in particular their reaction rates with O_3 and HO°, which involve different mechanisms of MP removal (see 2.3.2. Influence of the reaction rate of the compound with O_3 and HO°).

From equation 1, a chemical kinetic model can be deducted for the prediction of micropollutants abatement by ozonation (Elovitz and Von Gunten, 1999; Guo et al., 2018; Lee et al., 2014, 2013; Lee and von Gunten, 2016; Wang et al., 2018) :

$$-\boldsymbol{ln}\left(\frac{\boldsymbol{M}}{\boldsymbol{M_0}}\right) = \boldsymbol{k_{O_3}} \int [\boldsymbol{O_3}]\boldsymbol{dt} + \boldsymbol{k_{HO^\circ}} \int \left[\boldsymbol{OH^\circ}\right]\boldsymbol{dt} \quad [2]$$

Where:

- k_{O3} , $k_{HO°}$: second-order rate constant for the reaction of micropollutant (M) with O_3 and HO°
- $\int[O_3]dt$ and $\int[HO°]dt$: O_3 and HO° exposures, which are defined as the time-integrated concentration of O_3 and HO° over a given reaction period

Other species than molecular ozone and hydroxyl radicals play an important role in the mechanisms of ozone consumption (Westerhoff et al., 1997). As shown in Figure 2, a part of hydroxyl radicals does not react with micropollutants but with scavengers. The presence of scavengers depends on the matrix to treat (e.g. natural water, drinking water, and wastewater) (Buffle et al., 2006). It corresponds to some background water constituents, for instance carbonates (Yao et al., 2018). By scavenging hydroxyl radicals, some compounds can inhibit the ozone decomposition without producing hydrogen peroxide or superoxide radical ions. Other compounds can promote ozone decomposition by forming superoxide radical ions.

233 Water with natural organic matter will be consequently complex to model because of its
234 heterogeneity (Westerhoff et al., 1997) (see 2.2.1.) .

235

236 2.2. Influential parameters

237 2.2.1. Effect of matrix

238 The efficiency of ozonation process depends on the matrix to treat. For instance, water is a
239 complex mixture with a lot of different compounds, both organic and inorganic. They react

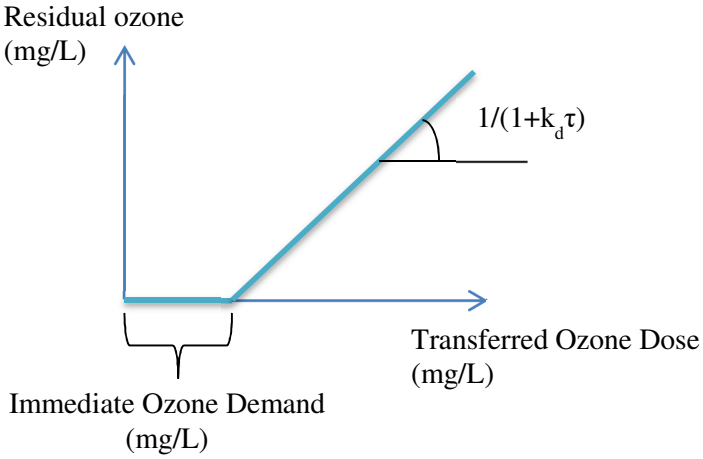

240 simultaneously, with molecular and free-radical mechanisms. Therefore, it is possible to
241 formulate the overall ozone consumption of water using two criteria. The first one is the
242 Immediate Ozone Demand (IOD), which represents the amount of ozone to apply before
243 detecting a measurable residue of ozone. It reflects very fast reactions of the natural organic
244 matter of the water with ozone. The higher the pH and the temperature of the water are, the
245 faster the ozone self-destructs. The second criterion is the slow consumption velocity. This is
246 defined by k_d, which is in this case a first order rate constant. In order to determine these two
247 characteristics, a graph (see Figure 3) can be drawn, representing the residual ozone in
248 function of the transferred ozone dose. The intercept of the straight line with the horizontal
249 axis gives the IOD, and the slope allows calculating $k_d\tau$, which is the Damköhler number
250 (Roustan et al., 1998) .

251 Figure 3: Determination of Immediate Ozone demand (mg/L) and k_d (min^{-1}), in a G/L
252 contactor operating continuously for the 2 phases, adapted from Roustan et al., 2003

253 For instance, for a surface water at 18°C, the IOD is about 0.4 gO_3/m^3 and the k_d about 0.18
254 min^{-1} (Roustan, 2003). Another example is provided by the works of Cruz-Alcalde et al.,

2019. The authors measured an average IOD of 16 mgO_3/L at the outlet of the biological treatment of 5 different WWTP.

Antoniou et al. predicted the ozone dose to be transferred to remove 42 pharmaceuticals. They found that the sensitivity of pharmaceuticals to degradation with ozone differs, depending on the target compound, but mostly on the matrix (i.e. the type of water) (Antoniou et al., 2013). Specifically, most of the difference is explained by the Dissolved Organic Carbon (DOC) of the water to be treated (Antoniou et al., 2013; Hansen et al., 2016). Antoniou et al. correlated the specific dose of ozone required to achieve reduction by one decade of each investigated pharmaceutical with the DOC of the effluent, which consumes a part of the dissolved ozone available by reacting with it.

2.2.2. Influence of the reaction rate of the compound with O_3 and HO°

As seen previously, the rate constant k_{O3} is a significant parameter for the ozonation efficiency. This parameter depends on the compound. A high second order reaction rate with O_3 leads to a good elimination of the pollutant. Yue et al. showed that compounds with a high k_{O3} were effectively removed with a rate superior to 95% with an ozone dose transferred varying between 0.3 and 1.5 mg/L, and a contact time of 8.6 min during pilot-scale experiments using a conventional ozonator (Yue et al., 2009). Bourgin et al. came to the same conclusions during conventional ozonation of surface water (i.e. Lake Zürich water, Switzerland). For instance, diclofenac and carbamazepine, with a k_{O3} superior to 10^4 $M^{-1}.s^{-1}$, were removed at more than 90% even for the lowest ozone dose transferred of 0.5 $mg.L^{-1}$ (Bourgin et al., 2017). Zimmermann et al. showed the same results within a gas bubble column. For substances reacting fast with ozone (e.g. diclofenac and carbamazepine, $k_{O3}=10^4$ $M^{-1}.s^{-1}$), they observed a good elimination for an ozone dosage transferred between 0.21 to 1.24 $g_{O3}.g_{Dissolved\ Organic\ Carbon}^{-1}$, except for the lowest dose (Zimmermann et al., 2011).

For compounds with a low to moderate reaction rate with O_3 (i.e. ozone resistant compounds with k_{O3} up to 10^1 $M^{-1}.s^{-1}$, and moderately ozone-resistant compounds with k_{O3} between 10^2 and 10^3 $M^{-1}.s^{-1}$), generally, oxidation increases with increasing ozone exposure and is influenced by the quality of the water matrix (Bourgin et al., 2017; Yue et al., 2009; Zimmermann et al., 2011). Yue et al. showed variable results. For instance, ibuprofen and clorfibric acid were removed between 3 and 62%. The same phenomena was observed for bezafibrate, which was removed between 28 and 99% under the same ozone exposure (Yue et al., 2009). Bourgin et al. found that sucralose (i.e. compound which only react with HO° and have a low reaction rate with O_3) was removed between 19 and 90%. The author also found that during conventional ozonation of resistant compounds, the abatement was moderate, even with a high ozone dose transferred of 3 $mg0_3.L^{-1}$ (Bourgin et al., 2017). In their work about transformation by-products of pharmaceutically compounds during drinking water ozonation, Tootchi et al. selected carbamazepine as pharmaceutical with a fast reaction rate with ozone and bezafibrate as pharmaceutical with a slow to moderate reaction rate with ozone (i.e. respectively over and under 10^4 $M^{-1}.s^{-1}$). The authors found that the major oxidation pathway for carbamazepine was the direct route (i.e. reaction with molecular ozone), while for bezafibrate it was both radical and molecular reactions (Tootchi et al., 2013).

2.2.3. Influence of operating parameters

Other parameters have an influence on the ozonation efficiency. For example, a higher pH promotes free radical mechanisms and causes a faster ozone decomposition because of the presence of hydroxide anions (Buffle et al., 2006; Mecha et al., 2016). A higher temperature leads to a better mobility of the water molecules and thus to a lower water viscosity and a higher water diffusivity. A higher ionic strength decreases the solubility of ozone and thus makes ozonation processes more difficult. The influence of these parameters is discussed later with more details in the specific case of membrane contactors (section 5).

2.3. Ozonation by-products

During the ozonation reaction, a low mineralization can occur (i.e. the oxidation could be incomplete). It conducts to the accumulation of intermediates, which are degradation by-products. These by-products in some cases, but not systematically, could be potentially more toxic than the initial contaminants (Gao et al., 2016; Gomes et al., 2017; Luo et al., 2014; Margot et al., 2013; Petala et al., 2008, 2006; Stalter et al., 2010a, 2010b; von Gunten, 2003a).

Several by-products can be cited as examples, like the NDMA (i.e. N-Nitrosodimethylamine), or the formaldehydes, which are produced by the reaction between ozone and natural organic matter (Hollender et al., 2009; Richardson, 2003; Samadi et al., 2015; Wert et al., 2007).

According to Gao et al., the products of parabens after reaction with hydroxyl radicals have a higher toxicity to green algae than the original paraben. They showed that when the alkyl-chain length of the parabens increases, the ecotoxicity of the degradation products also increases (Gao et al., 2016).

Bromates are other degradation by-products. They are formed during the ozonation of bromide-containing waters, such as river waters (Nobukawa and Sanukida, 2000; von Gunten, 2003a). Bromates are potentially carcinogenic and are not removed in biological filtration processes. Moreover, it is the only ozonation by-product regulated in drinking water (Merle et al., 2017; von Gunten, 2003a). Therefore, a lot of studies about water ozonation focus on this compound. A limit was established by the European Union at 10 µg/L in drinking water, but with the recommendation for the member states of having a lower value if possible (AIDA, 1998).

The bromate-forming mechanism is described in the Figure 4. In order to minimize bromates' formation, several solutions can be considered.

Figure 4: Bromate formation – chemical pathway, adapted from von Gunten, 2003b

The first one is an ammonia (NH_3) addition. NH_3 does not alter the ozone stability, and therefore does not interfere with oxidation processes. NH_3 reacts with HOBr, which is an important intermediate of the bromates' formation. Adding NH_3 leads to a lower bromates' formation up to a certain concentration of ammonia (except during the initial phase of ozonation in which it has no influence). No improvement is noticed beyond this limit. A balance between HOBr and NH_3 is established, which always leaves a fraction of HOBr, transformed then into BrO_3^- (i.e. bromates). This method is therefore not efficient with waters that already have a medium or high level of ammonia (von Gunten, 2003b) .

A second solution to minimize bromates' formation is a pH depression. This method

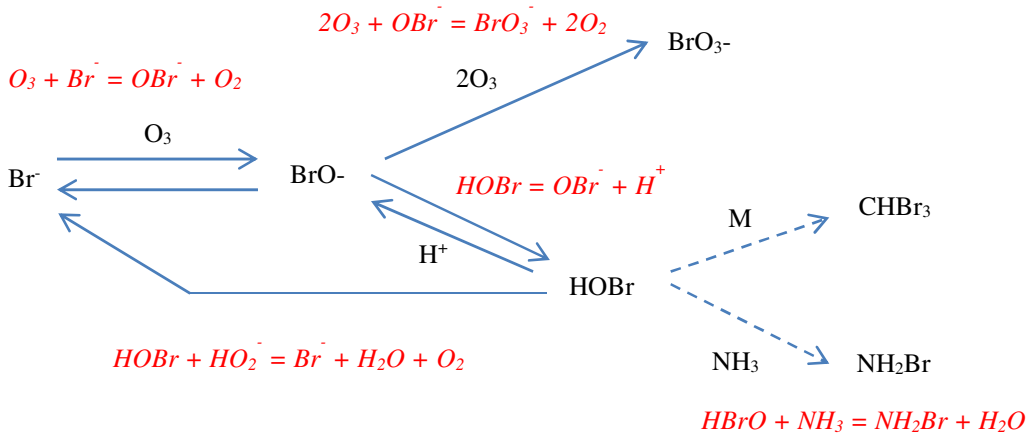

influences bromates' formation by shifting the balance between HOBr and OBr^- toward HOBr. When the pH decreases, hydroxyl radicals' exposure decreases as well, leading to a smaller overall oxidant exposure (i.e. ozone and hydroxyl radicals' exposure) and a lower bromates' formation. In the same way as the solution of ammonia addition, this solution does

not reduce the initial fast bromates' formation, which is almost independent of the pH (von Gunten, 2003b).

3. Generalities on membrane contactors with hollow fibers

3.1. Principle of a G/L membrane contactor with hollow fibers

In gas/liquid membrane contactors, the membrane acts as an interface between two phases. In contrast with membranes used for filtration, membrane contactors are non-selective (i.e. they don't offer any preference between compounds). The phases could be liquid/liquid or gas/liquid. The phases are keeping separated. The operation is bubbleless, thus the transfer takes place mainly by diffusion and not by dispersion of one phase into another. The driving force of the transfer is the concentration gradient. However, the pressure gradient have to be taken carefully to keep the interface at the entrance of the pores (Gabelman and Hwang, 1999) and thus avoid some problems with the membrane.

Depending on the membrane material, the fluids, and the operational conditions, the interface could be on one side or the other of the membrane, and sometimes inside. For a gas/liquid system and a hydrophobic membrane, the phase that fills the pores is the gas one. For a hydrophilic membrane, the liquid phase fills the pores. The best configuration for the diffusion of ozone is described in a next part.

Membranes could be made with organic (polymers) or inorganic (ceramic) materials. The selection of the material is made according to the future use of the membrane contactor, the fluids to keep in contact, the desired fluxes, etc.

According to several sources about gas absorption membrane contactor (Al-Saffar et al., 1995; deMontigny et al., 2006; Dindore et al., 2005; Li et al., 2010), counter-current mode

364 performs better than co-current mode. According to DeMontigny (deMontigny et al., 2006),
365 counter-current mode can be up to 20% more efficient than co-current mode.

366

367 3.2. Mass transfer using membrane contactors

368 As described by Bamperng et al. (see Figure 5), the absorption of a gas into the liquid phase is
369 broken down into several parts (Bamperng et al., 2010). The first is a transport of the
370 interested gas from the bulk of gas to the interface, between gas phase and a membrane. The
371 second is the transport of gas through the membrane pores. The last part is the dissolution of a
372 gas component into a liquid, eventually with a chemical reaction in addition which accelerates
373 the transfer.

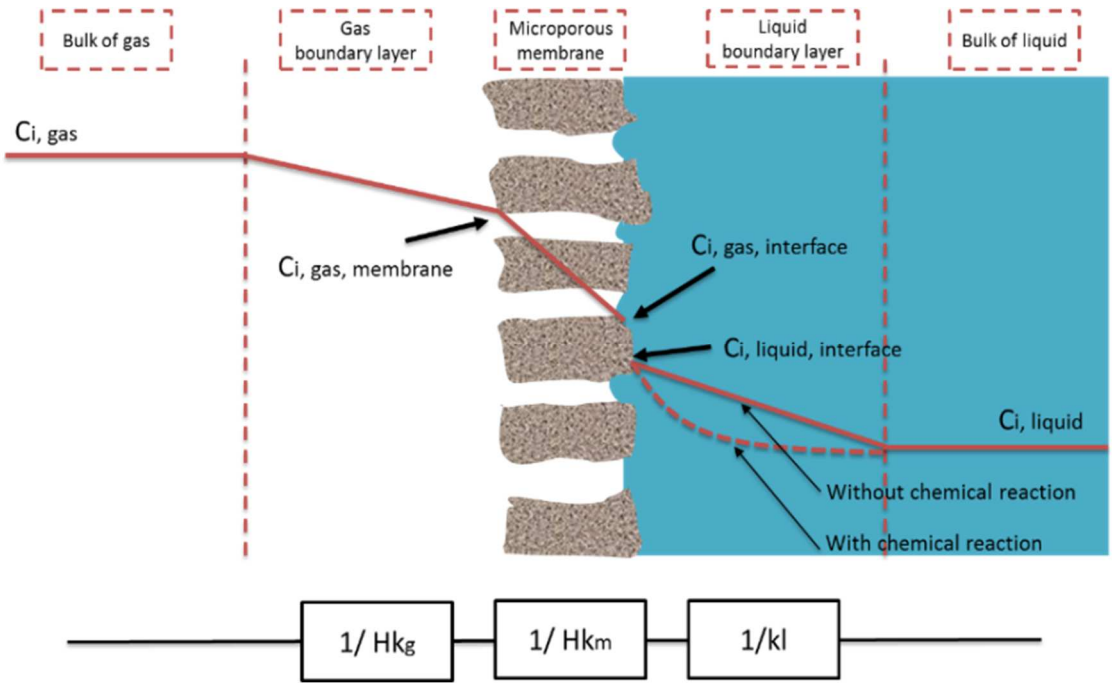

374

375 Figure 5 : Mass transfer regions and resistance-in-series in non-wetted membrane contactor,
376 adapted from Atchariyawut et al., 2007

377

3.2.1. Henry's law

At the interface between the 2 phases, the Henry's law is applicable if the following assumptions are respected. The solute (i.e. here the ozone) has to be slightly soluble in the solvent ($x_{O3} < 0.05$) and the gas phase is assumed to be perfect (moderate pressure and a temperature far from the condensation temperature) (Roustan, 2003).

$$\boldsymbol{C_i = K_{Hi} \cdot p_i} \quad [3]$$

According to this law, dissolved gases concentrations (C_i in mol/L) are proportional to the partial pressure of the gas in the air (p_i in hPa), depending on the dissolution constant of the gas (K_{HI} in $mol.kg^{-1}.hPa^{-1}$ or $mol.L^{-1}.hPa^{-1}$). Henry's law constant depends on the compound and can be expressed in several ways, and thus in several units.

3.2.2. The membrane mass transfer coefficient

The membrane mass transfer coefficient k_m is defined by the following relation, using the membrane structure properties:

$$\boldsymbol{k_m = \frac{D_g \times \varepsilon_m}{\tau_m \times l_m}} \quad \text{(Mavroudi et al., 2006) [4]}$$

Where:

- k_m : Mass transfer coefficient in the membrane ($m.s^{-1}$).
- D_g : Diffusion coefficient in the gas phase ($m^2.s^{-1}$)
- ε_m: Membrane porosity (dimensionless)
- τ_m : Membrane tortuosity (dimensionless)
- l_m : Membrane thickness (m)

3.2.3. Molar flux

The molar flux of the compound of interest (i.e. here the ozone) at the gas side can be expressed by:

$$\boldsymbol{J_i = k_g \times \left(C_{i,gas} - C_{i,gas,interface}\right)}$$ (Berry et al., 2017) [5]

Where:

- J_i : Molar flux of the compound of interest across the membrane ($mol.m^{-2}.s^{-1}$)
- k_g: Mass transfer coefficient in the gas ($m.s^{-1}$).
- $C_{i,gas,interface}$: Concentration of the compound of interest at the interface on the gas side ($mol.m^{-3}$)
- $C_{i,gas}$: Concentration of the compound of interest in the gas bulk ($mol.m^{-3}$)

The molar flux across the membrane can be described by:

$$\boldsymbol{J_i = k_m \times \left(C_{i,gas,membrane} - C_{i,gas,interface}\right)}$$ (Berry et al., 2017) [6]

Where:

- $C_{i,gas,membrane}$: Concentration at the gas-membrane interface ($mol.m^{-3}$), which can described by $C_{i,gas,membrane} = C_{,i,gas,interface}/S$, where S is the solubility of the gas in the membrane. Some studies assumed that $C_{i,gas,membrane}=C_{i,gas}$ (i.e. the concentration at the gas-membrane interface) is continuous (Pines et al., 2005; Shen et al., 1990).
- $C_{i,gas,interface}$: Concentration at the membrane-liquid interface on the membrane side ($mol.m^{-3}$), which can described by $C_{i,gas,interface}=C_{i,liquid,interface}$ x He, where He is the Henry's law constant (dimensionless, as described in [7]) and $C_{i,liquid,interface}$ is the concentration at the membrane-liquid interface on the liquid side.

The molar flux at the liquid phase side is described in the following equation.

$$J_i = k_L \times \left(C_{i,liquid,interface} - C_{i,liquid}\right)$$ (Berry et al., 2017) [8]

Where:

- k_L: Mass transfer coefficient in the liquid ($m.s^{-1}$)
- $C_{i,liquid,interface}$: Concentration of the compound of interest at the interface on the liquid side ($mol.m^{-3}$)
- $C_{i,liquid}$: Concentration of the compound of interest in the liquid bulk ($mol.m^{-3}$)

Therefore, thanks to the previous equations, the following formula can be used to express the molar flux from the overall mass transfer coefficient (Berry et al., 2017).

$$J_i = K_L \times \left(\frac{C_{i,gas}}{S} - He \times C_{i,liquid}\right)$$ [9]

Where K_L is the overall mass transfer coefficient ($m.s^{-1}$) described in the following section (see 3.2.4).

The mass balance on the liquid phase for steady state conditions can be described by:

$$\frac{dC_{i,liquid}}{dx} = \frac{1}{u_{L,mean}} K_L a \times \left(\frac{C_{i,gas}}{S} - He \times C_{i,liquid}\right)$$ (Berry et al., 2017) [10]

Where:

- a : Surface area of membrane per volume of liquid ($m^2.m^{-3}$)
- x : Direction of the flow (m)
- $u_{L,mean}$: Mean liquid velocity ($m.s^{-1}$)

Integrating the previous equation leads to the following relation, allowing the calculation of the theoretical K_La. The boundary conditions are such that the concentration of the compound of interest (i.e. the ozone) at the liquid inlet (i.e. x=0) is zero, and is equal to $C_{i,liquid,out}$ at the liquid outlet (i.e. x=L, representing the membrane length):

$$\frac{K_L a.L}{u_{L,mean}} = \frac{1}{He} ln\left(\frac{\frac{C_{i,gas}}{S}}{C_{i,gas} - He \times C_{i,liquid,out}}\right) \text{ [11]}$$

3.2.4. The overall mass transfer coefficient

The total resistance can be described by the resistance in series model, by analogy to Ohm's Law:

$$\frac{1}{K_L \times A_{outer}} = \frac{1}{S \times k_g \times A_{inner}} + \frac{1}{k_m \times A_m} + \frac{He}{k_L \times A_{outer}} \text{ (Berry et al., 2017) [12]}$$

Where:

- K_L : Overall mass transfer coefficient ($m.s^{-1}$)
- k_m, k_g, k_L: Mass transfer coefficient, respectively in the membrane, in the gas, and in the liquid ($m.s^{-1}$). When a chemical reaction occurs in the liquid, k_L can be replaced with $k_L = \frac{k_L^r}{E}$., such as $E = \frac{J_{O3} \text{ with reaction}}{J_{O3} \text{ without reaction}}$. E is called the enhancement factor and takes into account the effect of the reaction, which increases the concentration gradient and therefore the transfer speed at the interface (see Figure 5) (Nguyen, 2018). E can also be described in terms of Hatta number and instantaneous enhancement factor.
- A_{outer}, A_m, A_{inner}: Respectively the outer, logarithmic mean, and inner surface of the membrane (m^2)
- S: Solubility (e.g. of ozone) in the membrane material (dimensionless)

- He: Solubility (e.g. of ozone) in water (dimensionless). He can be described by the following equation.

$$\boldsymbol{He} = \frac{\mathbf{1}}{\boldsymbol{\alpha}} = \left(\frac{\boldsymbol{C_{O3,G}}}{\boldsymbol{C_{O3,L}}}\right)_{\boldsymbol{eq}} \text{(Roustan, 2003) [13]}$$

This equation is one form of the Henry's law. For the dissolution of ozone in water at 295K, the Henry's constant is 3.823 (mg/L)/(mg/L) (Atchariyawut et al., 2009). At 293K, this same constant is reduced to 2.907 (Roustan, 2003).

For hollow fibers membranes where the gas flows inside the fibers and the liquid outside, the previous equation becomes $\frac{\mathbf{1}}{\boldsymbol{K_L}} = \frac{\boldsymbol{d_o}}{\boldsymbol{S}\times\boldsymbol{k_g}\times\boldsymbol{d_i}} + \frac{\boldsymbol{d_o}}{\boldsymbol{k_m}\times\boldsymbol{d_{ln}}} + \frac{\boldsymbol{He}}{\boldsymbol{k_L}}$, where d_i, d_{ln}, d_o are respectively the inner, logarithmic mean, and outer diameters of the fibers (m).

4. Membrane materials

4.1. Membrane materials for gas/liquid membrane contactors

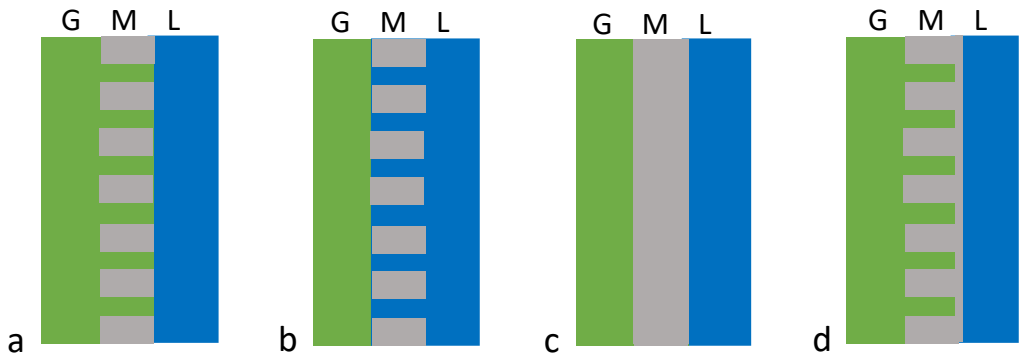

4.1.1. Microporous/dense membrane

Figure 6: Membrane configurations (a. non-wetted porous membrane, b. wetted porous membrane, c. dense membrane, d. composite membrane), adapted from Nguyen et al., 2011

The material of the membrane affects its performance and has to be chosen according to its application. Properties of the membrane, especially the pore size and the surface porosity,

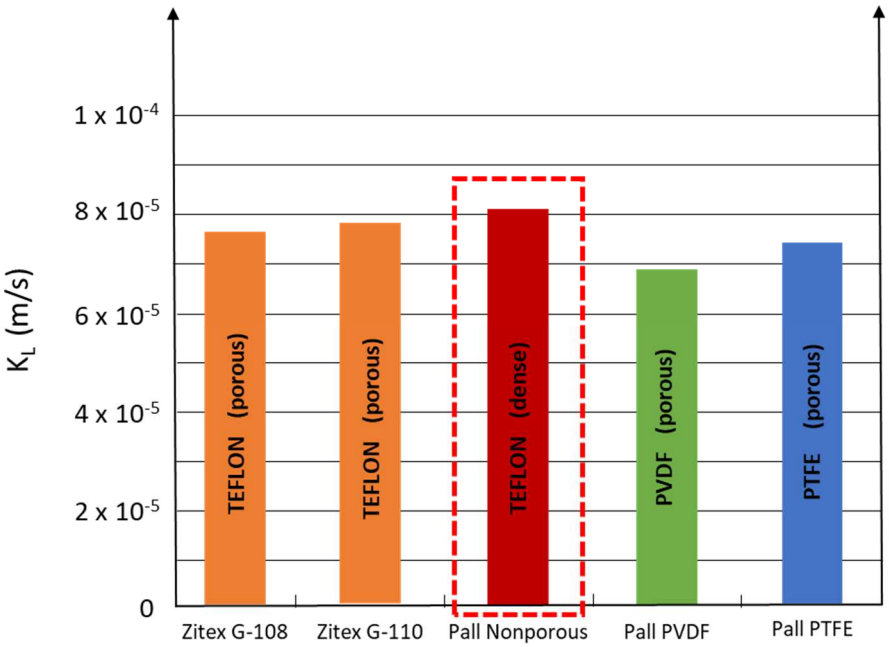

influence the transfer rate. Membranes can be classified in 3 categories: dense, porous, or composite (see Figure 6). According to Bakeri et al., the higher the pore size is, the higher the membrane mass transfer coefficient is (i.e. resistance within membrane is higher in dense membrane than in microporous) (Bakeri et al., 2012). Yet, higher pores increase the risk of wetting, which reduces the transfer quickly (Bakeri et al., 2012). Therefore, the operating pressure can be higher with dense membrane than with microporous because no bubbles are formed (i.e. no risk of bubbling). However, during their experiments, Pines et al. found a global mass transfer coefficient comparable between a Teflon nonporous membrane (i.e. a dense membrane) and different porous membranes (see Figure 7). The porous membranes used in this work were made with Teflon, PVDF, or PTFE. The pore volume was from 45 up to 55%. The pore size was from 0.5 up to 5 µm, and membrane thickness from 0.102 to 0.254 mm. (Pines et al., 2005)

Figure 7: Global mass transfer coefficient at liquid side Reynolds number of 2000 for different materials, adapted from Pines et al., 2005

487 According to Nguyen et al., a dense material can compete with classical porous membrane
488 contactors materials, depending on the dense skin thickness (i.e. it can have the same mass
489 transfer coefficient in the membrane) (see Figure 8). In their work, the authors highlighted the
490 interest of composite fibers for the CO_2 absorption. The fibers were fabricated from porous
491 polymers as supports and coated with dense permeable (here to CO_2) materials. The use of a
492 dense or a composite membrane seems therefore to be a possible solution to avoid bubbling
493 and wetting problems (i.e. transmembrane pressure limitations), without minimizing the
494 global mass transfer. (Chabanon and Favre, 2017; Nguyen et al., 2011)

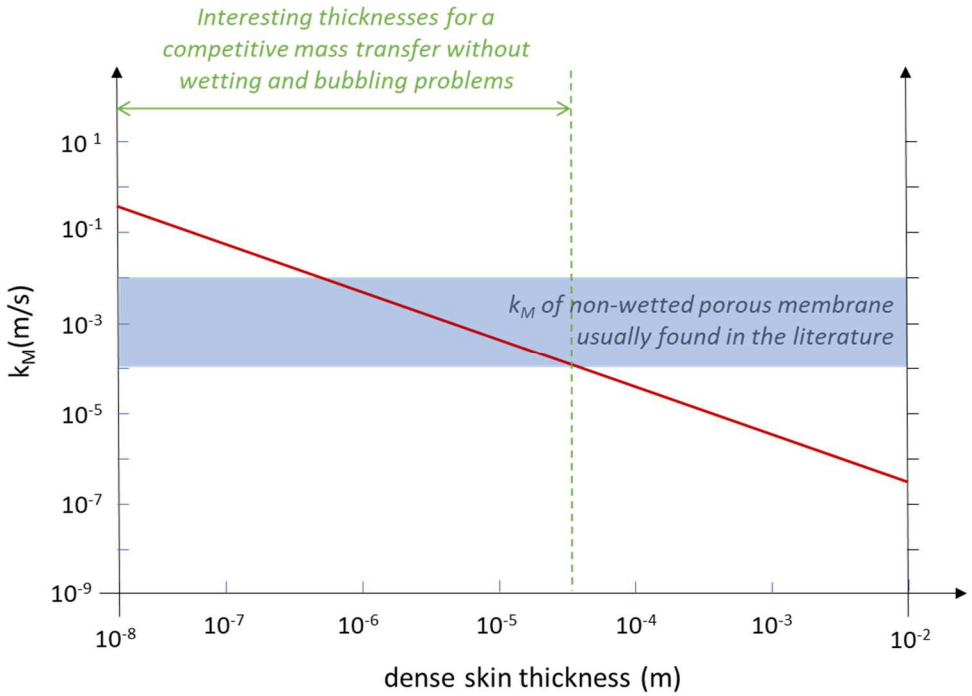

495 Figure 8: Effective mass transfer coefficient of a dense skin layer versus the layer thickness
496 for a polymer permeability of 500 Barrer, adapted from Nguyen et al., 2011

497 4.1.2. Advantages and disadvantages of organic membranes used in membrane
498 contactor

499 Table 2 summarizes the advantages and disadvantages of various organic materials which can
500 be used for membrane contactor.

Family	Abbreviation	Material	Characteristics	Advantages	Disadvantages	Sources
Polyolefins and fluoropolymers	**PVDF***	Polyvinylidene fluoride	Hydrophobic. Semi-crystalline (4 different crystalline forms with for each different mechanical and chemical resistances). Less hydrophobic than PTFE, but more hydrophobic than the other materials presented here. Degradation temperature between 375 and 400°C, and thus appropriate for water treatment.	Thermal stability, resistant to most of the corrosive chemicals and organic compounds. More resistant to ozone than PP. Better ozone flux than with PTFE for a same Reynolds number (liquid), but lower flux at long-term (after a couple of hours).	Sensitive to adsorption	(Bamperng et al., 2010; Choi and Kim, 2011; Khaisri et al., 2009; Mori et al., 1998)
	PTFE*	Polytetrafluoroethylene	Hydrophobic (contact angle between water and membrane at 110° for a PTFE dense film). More hydrophobic than PVDF.	High thermal and chemical stability (resistant to solvents and oxidizers). More resistant to ozone than PVDF.		(Khaisri et al., 2009; Mori et al., 1998)
	PE	Polyethylene	Hydrophobic	High thermal and chemical stability (resistant to solvents and oxidizers)		(deMontigny et al., 2006; Drioli et al., 2006)
	PP	Polypropylene				
Polysulfones	**PES** **PSu**	Polyether sulfone Polysulfone	Less hydrophilic than cellulose acetate Contact angle between water and membrane at 73°	High thermal and chemical stability, stable at a wide range of pH values, resistant to chlorine.	Risk of fouling by adsorption	(Drioli et al., 2006) (Zhang et al., 1989)
Cellulose and its chemical derivatives	**CA**	Cellulose acetate (di or tri)	Hydrophilic	Low fouling, high permeability to water, good selectivity.	Low thermal and chemical stability (especially to basis and chlorine)	(Mark, 1999; Zhang et al., 1989)
Polyamides ands Polyimides	**PA**	Polyamide	Low permeability to water (use for nanofiltration and reverse osmosis membranes)	High thermal, chemical, and mechanical stability, good selectivity.	Sensitive to chlorine, risk of fouling by adsorption of proteins	(Kwon et al., 2012, 2011)

501

502 Table 2: Synthesis of the different organic materials used in membrane contactors (* Material resistant towards ozone)

503 ## 4.2. Membrane materials used for ozonation with membrane contactors

504 ### 4.2.1. Organic/inorganic membrane

505 Organic membranes are made with polymers. They are often used because of the possibility to
506 modulate their intrinsic properties (e.g. mechanical, thermal, selectivity, etc). These
507 membranes can be prepared by sintering, stretching, track-etching, phase inversion, or other
508 ways. A material often used with ozone is for instance the PVDF (i.e. polyvinylidene fluoride)
509 (Atchariyawut et al., 2007; Bamperng et al., 2010; Jansen et al., 2005; Khaisri et al., 2009;
510 Leiknes et al., 2005; Pines et al., 2005).

511 Inorganic membranes are made with ceramic, metals, glass, or zeolite. They can be porous
512 (e.g. ceramic) or dense (e.g. made with metals or glass). Ceramics are the major class of
513 inorganic membranes. These membranes are prepared by mixing a metal (e.g. aluminium,
514 titanium, silicium, zirconium) with a non-metal (i.e. nitride, oxide, or carbide). They are
515 prepared by sintering or sol-gel processes, and have a great thermal, chemical, and
516 mechanical stability (Mulder, 1996). Membranes can also be hybrid (i.e. composed with both
517 organic and inorganic materials).

518 Ceramic membranes could be a good alternative for membrane contactors in comparison to
519 organic membranes because of their chemical, thermal, and mechanical stabilities. They seem
520 therefore to be an appropriate material for the use of ozone, which is a strong oxidant.
521 However, those membranes have hydrophilic properties due to the presence of hydroxyl
522 groups on their surface, and thus water is able to penetrate in their pores resulting in a higher
523 mass transfer resistance (Bamperng et al., 2010; Stylianou et al., 2016). Consequently,
524 ceramic membranes have a lower mass transfer coefficient compared to hydrophobic organic
525 membranes. The surface of ceramic membranes can be modified by grafting hydrophobic
526 compounds in order to solve this problem. The ozone mass transfer of such membranes may

527 be 5 times higher than non-grafted ceramic membranes (Picard et al., 2001). In the
528 experiments of Kukuzaki et al., the authors used shirasu porous glass (i.e. as membrane),
529 coated with nonafluorohexyltrichlorosilane (i.e. a highly hydrophobic compound). The ozone
530 mass transfer coefficient of these membranes was higher than the one of non-coated
531 membranes (i.e. the overall mass transfer coefficient was about 10^{-6} m/s for the hydrophilic
532 non-coated membranes and about 10^{-5} m/s for the hydrophobic coated membranes) (Kukuzaki
533 et al., 2010).

534 Other disadvantages of ceramic membranes have to be considered. Ceramic membranes have
535 a higher cost than polymeric counterparts (i.e. ≥ \$1,000 /m² versus \$100/m², respectively for
536 the ceramic versus the polymeric membrane material), due to higher production costs and
537 expensive starting materials (Amin et al., 2016; Ciora and Liu, 2003). However, the
538 membrane performance stability can be assured because of a higher cleaning efficiency with
539 harsh chemical if necessary (thanks to better chemical and thermal resistances). Therefore,
540 ceramic membranes have less fouling propensity, and thus a longer operational life, making
541 the cost of ceramic membranes more competitive (Ciora and Liu, 2003; Guerra and
542 Pellegrino, 2013).

543 Moreover, another drawback is the higher inner diameter of the ceramic in comparison to
544 polymeric membranes, leading to a lower surface area per unit volume. Tubular membranes
545 (i.e. internal diameter between 5 mm and 15 mm) and capillary membranes (i.e. internal
546 diameter between 0.5 mm and 5 mm) can be produced with ceramic materials, but hollow
547 fibers (i.e. internal diameter < 0.5 mm) are tougher to obtain, unlike with polymeric materials
548 (Amin et al., 2016).

4.2.2. Hydrophobic/hydrophilic membrane

As explained before, pores are filled with liquid in hydrophilic membranes while they are filled with gas using a hydrophobic membrane. Ozone and oxygen diffusion are higher in gas than in water, thus the membrane resistance is lower with a hydrophobic membrane. However, wetting and condensation problems may occur, unlike with hydrophilic membrane (see 5.1 Transmembrane operating pressure (TMP) using membrane as gas/liquid contactor).

4.2.3. Sustainability

The sustainability of membrane material under highly reactive character of ozone is one of the main challenges of using a membrane contactor for ozonation.

Bamperng et al. compared a membrane contactor with PVDF material to a membrane contactor with PTFE material, for the ozonation of dye wastewater. They found that PTFE has a better sustainability because its performance was barely reduced, while PVDF lost 30% of its initial performance within a few hours (Bamperng et al., 2010). Dos Santos et al. investigated the resistance to ozone oxidation of organic (i.e. polymeric) membranes in order to select the best material to use in ozonation process for water treatment. The authors showed that materials with electrophilic atoms attached to the carbon in the polymer backbone (e.g. PVDF and PTFE) have a good resistance to ozone. They observed that membranes with single C-C or Si-C bonds (e.g. PP and PDMS) also have a good resistance to ozone but showed structural modifications after a long period of use. Lastly, materials with carbon-carbon double bonds (e.g. PEI and PES) were highly degraded (Alves dos Santos et al., 2015).

5. Ozonation using membrane contactors

In this review, experiments using oxygen as gas (instead of ozone) have also been taken into account as oxygen and ozone are oxidizing gas, and have a relatively similar behavior.

572 5.1. Transmembrane operating pressure (TMP) using membrane as gas/liquid contactor

573 If the pressure of the liquid is too high, membrane could be wetted (i.e. the liquid phase
574 penetrates into the membrane pores and the membrane loses its hydrophobicity), creating a
575 stagnant film which interferes with the transfer. The transfer is therefore better when the
576 gas/liquid interface is kept at the membrane surface. Moreover, ozone diffusivity is better
577 inside the gas than inside the liquid, and thus ozone transfer is promoted when the interface is
578 located on the liquid side of the membrane. It highlights the importance of the material used,
579 especially its hydrophobicity (Goh et al., 2019; Picard et al., 2001; Xu et al., 2019).

580 Picard et al. quantified the influence of the membrane's humidity. The authors studied the
581 drying time of wet membranes before an experiment, and made a correlation with the transfer
582 rates obtained. They concluded that water inside the membrane pores is a major limiting
583 factor to the transfer (Picard et al., 2001). The maximum pressure to avoid this phenomenon is
584 called the breakthrough transmembrane pressure, or the liquid entry pressure of water
585 (LEPw), or the wetting pressure (Choi and Kim, 2011; Smolders and Franken, 1989). It is
586 defined by Laplace equation such as $EPw = -\frac{B\gamma_L}{d_p}$, with dp the diameter of the largest pore,
587 B the form factor of the pore, and γ_L the superficial tension of the liquid (Xu et al., 2019). In
588 order to determine the LEPw of a membrane, the method described by Smolder and Franken
589 can be used (Smolders and Franken, 1989)(Choi and Kim, 2011). This consists of applying a
590 slight pressure in the liquid phase of about 0.3 x 10^5 Pa, during at least 10min. Then, the
591 pressure is increased by step of 0.68 x 10^3 Pa. The LEPw is reached when a continuous flow
592 is observed in the permeate side (i.e. in the gas phase).

593 The liquid pressure has to be higher than the gas pressure, in order to avoid bubbling (i.e.
594 cross of bubbles in the liquid side), but lower than the breakthrough transmembrane pressure.
595 This TMP depends on the membrane pore size: small pores allow higher pressure. For

596 instance, microporous membranes have a breakthrough transmembrane pressure of about 20
597 kPa. (Fang et al., 2004)

598 5.2. Effect of several parameters on mass transfer

599 5.2.1. Effect of liquid velocity

600 Ozone flux increases with increasing liquid velocity (Atchariyawut et al., 2009; Bamperng et
601 al., 2010; Pines et al., 2005; Stylianou et al., 2016; Zoumpouli et al., 2018). In the
602 experiments of Atchariyawut et al., Bamperng et al., Pines et al., Stylianou et al., and
603 Zoumpouli et al., ozone flowed through the shell side and the liquid through the tube side (i.e.
604 inside the fibers). Ozone flux was calculated from a mass balance in the gas phase or in the
605 liquid phase. Concentration gradient is the driving force for the ozone transfer into the
606 membrane. When the liquid flow velocity increased, the resistance to ozone transfer at the
607 interface between the gas and liquid phases decreased (i.e. the liquid mass transfer coefficient
608 kL increases). The concentration difference was maintained high and thus higher ozone flux
609 could be transferred. This trend was demonstrated for both porous and non-porous
610 membranes. According to Zoumpouli et al., liquid flow velocity is the dominant parameter for
611 ozone transfer, followed by membrane thickness and ozone gas concentration (Zoumpouli et
612 al., 2018). However, it must be noticed that in these experiments, the impact of other
613 parameters (e.g. the pH) was not investigated.

614 For practical applications, it seems interesting to keep a high liquid velocity to have a high
615 mass transfer and to keep important shear forces at the surface of the membrane that could
616 decrease a possible fouling. However, higher liquid velocity implies lower residence time. For
617 many applications, it is important to reach a given value of dissolved ozone concentration in
618 order to get sufficient kinetic reaction or good disinfection level. As a consequence, a

compromise between high liquid velocity (i.e. high transfer) and high dissolved ozone concentration should be found.

5.2.2. Effect of gas

5.2.2.1. Gas velocity

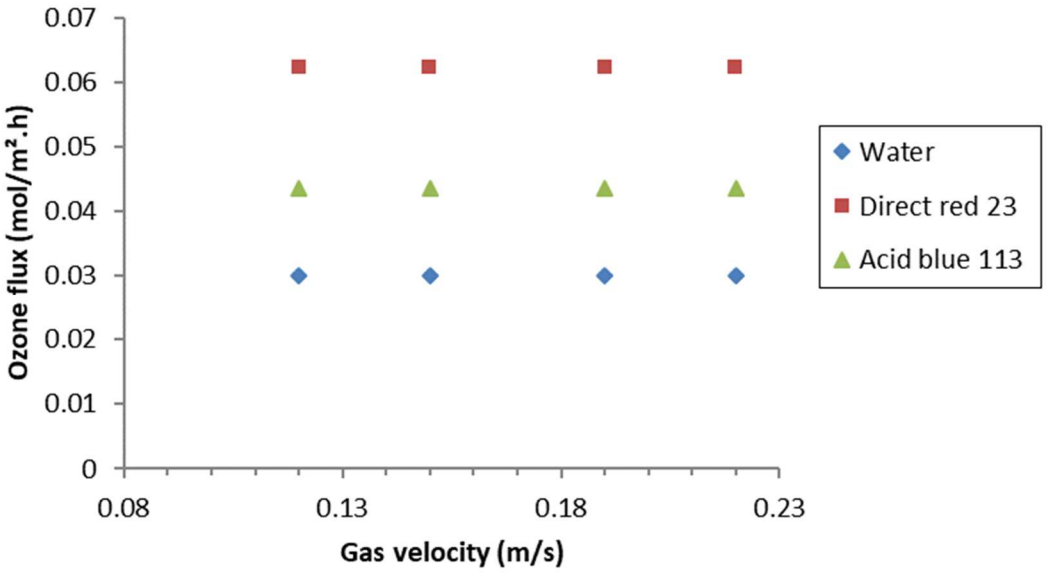

Figure 9: Ozone molar transfer flux as function of gas flow velocities with PVDF membrane at T=28°C, liquid phase velocity = 0,46 m/s, and initial dye concentration = 100 mg/L, adapted from Bamperng et al., 2010

Ozone flux is not influenced by gas velocity. The work of Bamperng et al (see Figure 9) showed that when gas velocity increases, ozone flux is not impacted (Bamperng et al., 2010). These experiments were made using water, direct red 23, and acid blue 113 (i.e. two dyes) and with a hollow fiber polyvinylidenefluoride (PVDF) membrane module. The ozone was produced with ozone generator by pure oxygen. The gas velocity varied between 0.12 and 0.22 m/s, and the ozone concentration was 40 mg/L. The liquid phase velocity was set at 0.46 m/s and the initial dye concentration was set as 100 mg/L. The ozone fluxes for pure water

were determined by mass balance in the liquid phase, and the ozone fluxes for dye solution by mass balance in the gas phase. Results showed that for both water and dye solution (i.e. the liquid phase), the ozone flux did not evolve with an increasing gas velocity.

As seen previously (5.2.1), ozone flux is influenced by liquid velocity, therefore the mass transfer resistance is in the liquid phase, and not in the gas phase (Atchariyawut et al., 2009, 2007; Bamperng et al., 2010; Berry et al., 2017; Khaisri et al., 2009). In addition, Pines et al. found that the resistance is higher in the liquid film than in the membrane (Pines et al., 2005).

5.2.2.2. Nature of the gas

According to Berry et al., unlike ozone, the mass transfer resistance of oxygen is located in the membrane (Schwarzenbach et al., 2006). Côté et al. showed that oxygen mass transfer coefficient was better with pure oxygen than with air (Côté et al., 1989). According to the authors, this difference in transfer comes from the formation of nitrogen bubbles (i.e. with air), which strip the oxygen. The bubbles are formed against the fibers, and then escape to the liquid side and its outside in the form of gas, since the water is initially saturated with nitrogen at atmospheric pressure. Thus, the mass transfer in a membrane contactor depends on the nature of the gas. These results were obtained with gas inside the fibers and liquid in the shell.

5.2.2.3. Concentration in the gas

When the concentration of ozone in the gas increases, the dissolved ozone concentration measured at the outlet of the contactor in the liquid phase also increases. Stylaniou et al. obtained the results represented in the Figure 10, at a liquid temperature of 20°C, with a hydrophobically modified α-Al_2O_3 ceramic membrane (Stylianou et al., 2016). It is important to note that the membrane used was tubular, which implies a larger diameter than with hollow

657 fibers (see 4.2.1). The ozone concentration was measured with potassium iodide method. The
658 authors made the same experiments for different temperatures (i.e. 15, 25, 30 and 30°C), with
659 different concentrations (i.e. 20, 40 and 60 mg/L). All the plots present the same trend as seen
660 in the Figure 10.

661 The concentration of a compound (e.g. ozone or oxygen) at the interface between gas and
662 liquid is linked to its partial pressure by Henry's law (see 3.2.1) with respect to its
663 concentration in the gas phase (i.e., $C_{interface} = \frac{C_{O3,gas}}{s}$ where s is the dimensionless partition
664 coefficient for ozone (Stylianou et al., 2016)). Therefore, when the concentration in the inlet
665 gas increases, partial pressure also increases. According to the results of Stylaniou presented
666 previously, the increase of partial pressure should raise the same way.

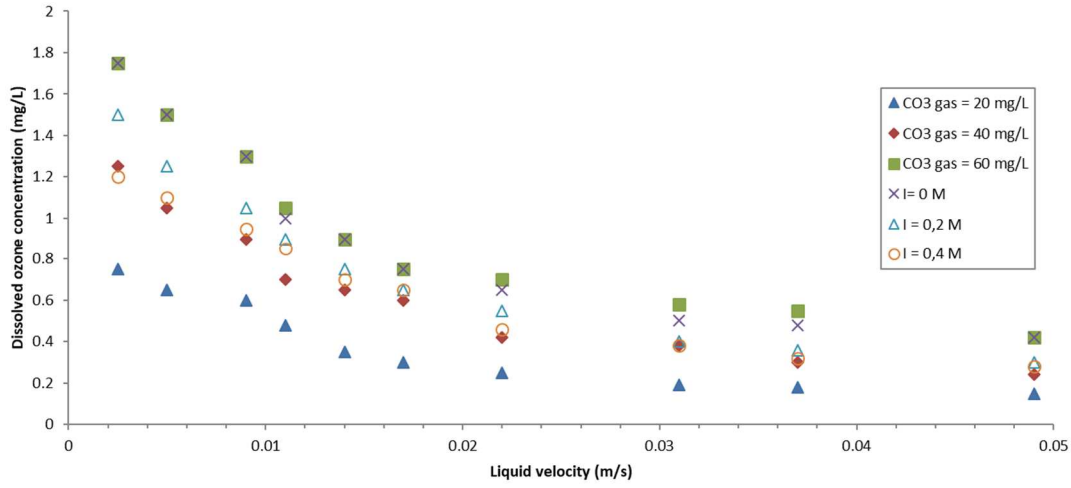

667

668 Figure 10: Dissolved ozone concentration at the outlet of the contactor for different ozone
669 concentration in gas phase and for several ionic strengths, in function of liquid velocity, at
670 20°C, adapted from Stylianou et al., 2016

671

5.2.2.4. Operating gas pressure and oxidant partial pressure

In the experiments of Côté et al. with dense hollow fiber membranes, the global mass coefficient K is independent of oxygen partial pressure up to 3 bars ($K=28.3 \times 10^{-6}$ $m.s^{-1}$) (Côté et al., 1989). However, at higher pressure, K dropped to 23.3×10^{-6} $m.s^{-1}$. Côté explained this drop with the apparition of micro-bubbles on the surface of the fibers. This phenomenon could be avoided with a higher water velocity, preventing the partial pressure from exceeding the saturation point. In contrast, Ahmed et al. showed in their studies that the mass transfer coefficient K increases with increasing operating pressure (Ahmed et al., 2004). The same result was obtained in previous studies (Ahmed and Semmens, 1992a, 1992b; Li et al., 2010). Li et al. found that, for hydrophilic treated polypropylene hollow fiber membranes, when the operating pressures increases from 20 to 100 kPa, the membrane resistance decreased almost linearly from 8.8×10^{-4} to 4.6×10^{-4} $s.m^{-1}$(i.d 1/K), giving a higher oxygen flux due to the higher partial pressure of oxygen (Li et al., 2010). These results go against Côté's conclusions. However, the same ultimate pressure beyond which bubbles appear was mentioned. It represents one of the limits of this process.

5.2.3. Effect of temperature

The experiments of Stylaniou et al. showed that temperature has a very little impact on the dissolved ozone concentration, compared to the influence of liquid velocity, pH, and ozone concentration values in the gas phase (Stylianou et al., 2016). However, temperature affects ozone diffusivity, decomposition rate constant, and ozone solubility in the water. At the interface, Henry's law is applicable (see 3.2.1), which depends on the temperature (Sotelo et al., 1989). When the temperature increases, water molecules have a greater mobility, and thus the viscosity of water decreases and its diffusivity increases (by around 1.2 times every 5°C according to Stylaniou et al.). As a consequence, the mass transfer coefficient in the liquid

696 phase raises. In the same way, when the temperature increases, lower energy is required for
697 the reaction between ozone and hydroxyl ions, and thus the ozone decomposition rate
698 increases (by around 1.5 times every 5°C). Conversely, ozone equilibrium concentration
699 decreases (by around 1.15 times) due to the decrease of gas solubility. Therefore, it seems
700 important to take this factor into account.

701 5.2.4. Effect of transfer direction

702 The majority of the studies about ozonation using a membrane contactor use the gas in the
703 shell side and the liquid inside the fibers. The main advantage of this configuration is a good
704 distribution of the dissolved ozone in the liquid, thus allowing a good treatment of the
705 pollutants. However, this configuration is more favorable to clogging. The circulation of the
706 liquid in the shell side greatly reduces this risk. Nevertheless, a risk of short circuit in the shell
707 appears, and therefore this configuration promotes the formation of areas without dissolved
708 ozone, in which the pollutants are not treated (i.e. there is a risk of mal-distribution of the
709 dissolved ozone and of channeling of the water in the carter (Dindore et al., 2005). According
710 to Wenten et al., the best configuration for iodide ozonation with a membrane contactor is the
711 one illustrated in the Figure 11 where the gas (ozone) passes through the tube side (i.e. inside
712 the fibers) and the liquid (acidic iodide) solution passes through the shell side (Wenten et al.,
713 2012). It corresponds to the configuration where the higher iodine concentration is obtained at
714 the outside of the system (i.e. the objective was to oxidize iodide into iodine). In their study
715 and for this configuration, the highest iodine concentration reached 300 mg/L, after a contact
716 time of 720s. For the other configuration, where the ozone was flowing in the shell side, the
717 highest concentration reached 35 mg/L, after a contact time of 1800s. According to the
718 authors, the difference between the two results can be explained by the reaction of the ozone
719 with the membrane material when the gas was running in the shell side. It causes the
720 transformation of the ozone into oxygen, which reacts very slowly with iodide.

721

722 Figure 11: Configuration of membrane contactor with internal/external ozone transfer

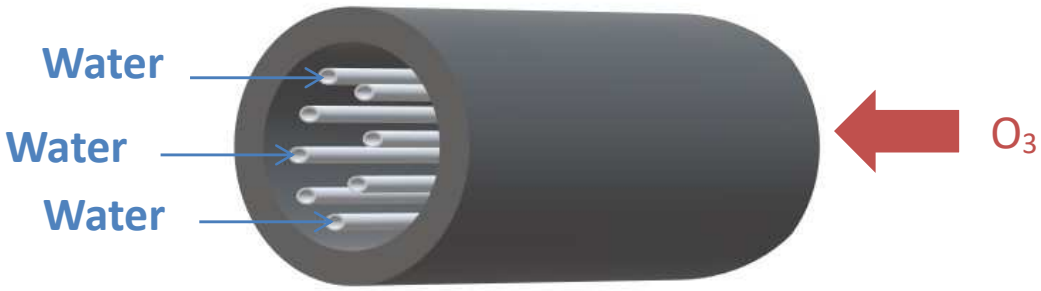

723

724 Figure 12: Configuration of membrane contactor with external/internal ozone transfer

725 5.2.5. Effect of chemical reaction

726 When the liquid used in the contactor is pure water, no chemical reaction takes place. In the
727 experiments of Stylaniou et al., ozone flux is lower with pure water than with surface water
728 (Stylianou et al., 2016). It can be explained by the concentration gradient, which is maintained
729 higher when ozone reacts with surface water, and in this case with micropollutants. According
730 to Roustan et al., with hollow fiber organic membrane, the mass transfer coefficient of oxygen

K_La is 6 times higher with fast reaction time in the liquid than without (i.e. 0.240 s^{-1} for 0.040 s^{-1} without) (Roustan, 2003). Therefore, the oxygen mass transfer is also 6 times higher with fast reaction than without. This is reflected in the mass transfer model with the several dimensionless numbers. The first one is the Hatta's number. It gives information on the competition between reaction and diffusion speed, inside the liquid film. It also indicates where the chemical reaction takes place. For a second order reaction (see 2.1, this number is defined by $\boldsymbol{Ha} = \frac{\sqrt{k_{O3} C_{i,liquid} D_{O3,L}}}{k_L}$, where $D_{O3,L}$ is the diffusivity of ozone in liquid phase ($m^2.s^{-1}$), $C_{i,liquid}$ is the concentration of the targeted compound in the liquid phase ($mol.m^{-3}$), k_L is the transfer coefficient in liquid phase ($m.s^{-1}$), and k_{O3} is the 2nd order reaction rate constant of ozone with the compound of interest ($m^3.\ mol^{-1}s^{-1}$). If Ha is small (i.e. Ha<0.3), the reaction is slow compared to the diffusion. If Ha is high (i.e. Ha>3), the reaction is fast compared to the diffusion.

The enhancement factor ($\boldsymbol{E} = \frac{\boldsymbol{Flux\ at\ the\ interface\ with\ chemical\ reaction}}{\boldsymbol{Flux\ at\ the\ interface\ without\ chemical\ reaction}}$) describes the importance of the chemical reaction on the mass transfer at the interface between the gas and liquid phase. If E=1, the reaction does not accelerate the transfer. If E>1, the reaction accelerates the transfer.

Another number is helpful to characterize the transfer, and to determine the material which reacted in the liquid film: the M criterion, such as: $= \frac{Flux\ between\ liquid\ film\ and\ bulk\ of\ liquid}{Flux\ at\ the\ interface\ between\ gas\ and\ liquid}$. When M=1, all the compound quantity transferred from the gas phase to the liquid phase is also transferred to the bulk of liquid. Therefore, the chemical reaction only takes place in the bulk of liquid and the reaction does not accelerate the mass transfer (i.e. E=1 and Ha<0.3). The concentration profile of the compound in the liquid film is linear. When M<1, the reaction takes place in both liquid film and bulk of liquid, and thus reaction accelerates the transfer (i.e. E>1 and Ha between 0.3 and 3). When M=0, all the compound in the liquid

phase reacts in the film. No molecule reaches the bulk of liquid. The reaction accelerates the transfer (i.e. E>1 and Ha>3).

5.2.6. Effect of pH

According to Wenten et al., pH of the liquid phase does not have a significant impact on the ozonation of iodide into iodine (Wenten et al., 2012). However, several studies revealed the opposite (Bamperng et al., 2010; Stylianou et al., 2016). Free radicals mechanisms are promoted with increasing pH and ozone decomposition is faster due to the presence of hydroxide anions. Therefore, ozone resistant compounds may react by indirect reaction thanks to the formation of hydroxyl radicals, which are non-selective oxidants. Simultaneously, ozone decomposition at higher pH keeps the ozone concentration gradient higher, and thus promotes the flux through the membrane.In their experiments on dye solutions, Bamperng et al. showed that the higher the pH solution was, the higher the ozone flux was (Bamperng et al., 2010). In the study of Stylaniou et al., the reaction rate constant increased with the pH increase (see Table 3) (Stylianou et al., 2016).

Table 3: Influence of pH on reaction order and rate constant of ozone decomposition at 20°C, adapted from Stylianou et al., 2016

pH	Reaction order n	Rate constant of ozone decomposition K′ (1/s·(L/mg)(n−1)) (±5%)
4	2	0,0017
6	2	0,0049
9	1	0,624

772 5.2.7. Effect of ionic strength

773 Stylaniou et al. investigated the effect of ionic strength on ozone flux (Stylianou et al., 2016).
774 Ionic strength was adjusted by the addition of NaCl solution. The authors made the same
775 experiments for different temperatures (i.e. 15, 25, 30 and 30°C), with different
776 concentrations (i.e. 0, 0.2 and 0.4 M). All the plots present the same trend as in the Figure 10,
777 where the dissolved ozone concentration at the outlet of the contactor decreases when the
778 liquid velocity increases. Zero ionic strength corresponds to the use of deionized water
779 without the addition of NaCl.

780 An increase of ionic strength decreases the solubility of ozone and thus also decreases the
781 equilibrium concentration of ozone at the interface between gas and liquid, as described by
782 Henry's law (see 3.2.1). The ionic strength has also an impact on the surface tension, and thus
783 on the allowable transmembrane pressure (see 5.1. Indeed, dissolved salts increase the surface
784 tension, and in the same way the breakthrough pressure.

785

786 5.2.8. Effect of surfactant

787 Côté et al. studied the impact of surfactant in liquid phase on the oxygen flux (Côté et al.,
788 1989). For these experiments, commercial soap containing 3.2% by weight of anionic
789 surfactant was added to the initial deoxygenated water. It appeared that the addition of soap
790 increased the mass transfer coefficient (i.e. 7% for a liquid velocity of 2.28 cm/s and 20% for
791 a velocity of 7.71 cm/s). According to the authors, it is a significant parameter because the
792 amount added (i.e. 190.5 mg/L) is equivalent to approximately 6 mg/L of surfactant (i.e.
793 lauryl sulphate), which is a concentration often observed in wastewater (Boon,
794 1980).Surfactants have an impact on the surface tension, and thus on the allowable

795 transmembrane pressure (see 5.1. Indeed, surfactants decrease the surface tension, and in the
796 same way the breakthrough pressure. Therefore, the risk of wetting is higher.

797 5.2.9. Effect of membrane material

798 The membrane material has a significant role in the mass transfer efficiency. As mentioned
799 above (see 3.1), membranes have to be porous in order to facilitate the transfer, and
800 hydrophobic to avoid the wetting phenomenon, which leads to the formation of a stagnant
801 film inside the membrane and thus to a reduced mass transfer. Ozone is a very strong oxidant,
802 and thus can attack the membrane material if this one is not sufficiently resistant. For an
803 application of ozonation with a membrane contactor, two materials stand out: the PVDF and
804 the PTFE which are the only organic membranes that can be used with ozone. According to
805 Bamperng et al., PTFE leads to a more stable and higher flux than PVDF for a long operation
806 period (i.e. few hours of use) (Bamperng et al., 2010).

807 5.2.10. Summary table of the effect of parameters on mass transfer

808 Table 4: Effect of parameters on mass transfer

Parameters	Range in litterature	Influence on the ozone transfer when the parameter increases	Sources
Liquid velocity	**0.002 - 0.9 m/s**	**+**	**(Atchariyawut et al., 2009; Bamperng et al., 2010; Pines et al., 2005; Stylianou et al., 2016; Zoumpouli et al., 2018)**
Gas velocity	**0.003 - 0.22 m/s**	**=**	**(Atchariyawut et al., 2009, 2007; Bamperng et al., 2010; Berry et al., 2017; Khaisri et al., 2009)**
Concentration of O3 in the gas	**20 - 60 mg/L**	**+**	**(Stylianou et al., 2016)**
Operating gas pressure	**6.9 - 413.7 kPa**	**+**	**(Ahmed et al., 2004; Ahmed and Semmens, 1992a, 1992b;**

			Li et al., 2010)
Temperature	**15 - 50°C**	**+**	**(Stylianou et al., 2016)**
pH	**4 - 9**	**+**	**(Bamperng et al., 2010; Stylianou et al., 2016)**
Ionic strength	**0 - 0.4 mol/L**	**-**	**(Stylianou et al., 2016)**
Surfactant	**0 - 6 mg/L**	**+**	**(Côté et al., 1989)**
Chemical reaction	**With or Without (pure water)**	**+ (With)**	(Stylianou et al., 2016)
Transfer direction	**In/Out or Out/In**	**+ (In/Out)**	**(Wenten et al., 2012)**

809

810 5.3. First results on micropollutants

811 During their experiments, Stylaniou et al. showed the technical feasibility of a membrane
812 contactor for the removal of various micropollutants in surface waters with diffusion of ozone
813 and peroxone (Stylianou et al., 2018). They studied the transformation of carbamazepine
814 (CBZ), benzotriazole (BZT), p-chlorobenzoic acid (pCBA), atrazine (ATZ), and the
815 formation of bromates in a ceramic tubular membrane contactor, where the gas was in the
816 shell side. The CBZ was removed at more than 90%, with a diminution of its concentration
817 below 0.1 µM at 0.4mgO_3/mgDOC. BTZ, pCBA, and ATZ was removed respectively at 70,
818 57, and 49%. The removal efficiency followed the reactivity order of the compounds with O_3.
819 The addition of peroxone reduced the elimination of CBZ by 8%, but increased the
820 elimination of ozone-resistant compounds (i.e. pCBA and ATZ) by about 5-10%.

821 In order to make a comparison between the different contacting ozonation processes, batch
822 experiments (i.e. conventional, prepared by continuously bubbling ozone and therefore O_3
823 saturated) and continuous experiments with ceramic tubular membranes having different inner
824 surface per volume were performed. The results for the CBZ (i.e. the ozone reactive
825 compound) were similar whatever the process. However, the hydroxyl radical exposure was
826 slightly higher in the conventional experiments for ozone and peroxone processes, which
827 leads to a better abatement of ozone-resistant compounds in the conventional process. Thus,

828 the authors suggest that using a membrane with a high inner surface per volume, like for
829 instance the hollow fibers, leads to a better efficiency of ozonation processes thanks to a more
830 uniform distribution of oxidants (i.e. ozone and peroxone) in the water to be treated.

831 Concerning the bromate formation, Stylaniou and al. showed that ozone concentration lower
832 than 20 mg/L are required to be under the regulated concentration limit of bromate (i.e. they
833 did not achieve this limit even at a concentration of 0.020 mg/L, which was the lowest
834 concentration used during their experiments). Indeed, European Commission and US EPA
835 defined this limit at 10 µg/L in drinking water (EC directive 98/83; USEPA,1998). The ozone
836 concentration is a very important parameter to minimize the formation of these compounds. In
837 their experiments, Stylaniou et al. found a high bromate concentration of 49 µg/L at 0.8
838 mgO_3/mgDOC with the ozone process. In these experiments, comparing with conventional
839 process, membrane processes led to a higher bromates' formation. To conclude, the authors
840 suggest that the use of membrane contactor with both a low ozone gas concentration and the
841 highest possible inner surface per volume are required to improve the micropollutants
842 abatement and to reduce the bromates' formation.

843 Merle et al. worked on a combination of a membrane contactor with advanced oxidation
844 process for the abatement of micropollutants and the minimization of the bromates' formation
845 (Merle et al., 2017). The authors used PTFE hollow fiber membrane. The water flowed inside
846 the fibers, and the gas inside the shell. They focused especially on bromates' production, and
847 studied the abatement of pCBA because of its high reactivity with hydroxyl radicals and low
848 reactivity with molecular ozone (i.e. ozone-resistant compound). Compared to the
849 conventional peroxone process (i.e. with bubbles), this process showed a better abatement of
850 micropollutants and less bromates formation, for groundwater and surface water treatment.
851 For instance, for a groundwater containing 180 $\mu g.L^{-1}$ of bromides and 0.48 $mgDCO.L^{-1}$, with
852 a hydrogen peroxide concentration of 5.67 $mgH_2O_2.L^{-1}$, and an ozone concentration in the gas

853 phase of 0.5 g.Nm^{-3}, an abatement of p-CBA of 95% was achieved after 300 s of residence
854 time, and less than 0.5 µg/L of bromates were produced. In the conventional process, 8 µg.L^{-1}
855 was formed under the same conditions. It can be noted that with a higher ozone concentration
856 in the gas phase (i.e. 1g/Nm^3, 2.5 g/Nm^3 and 10 g/Nm^3 in these experiments), the p-CBA
857 abatement was better and faster, but more bromates were produced.

858

859 **6. Modeling of ozone and oxygen mass transfer through membrane contactors for the**
860 **elimination of micropollutants**

861 Several studies have investigated the modeling of ozone and oxygen transport through
862 membrane contactors during ozonation processes, from the gas phase to the liquid phase.
863 Most of these works focused on applications such as CO_2 absorption, acid gas capture (i.e.
864 gas-liquid absorption), or liquid-liquid extraction (Faiz et al., 2013; Zhang et al., 2014).

865 The modeling of such processes is useful for a better understanding of the physical and
866 chemical phenomena occurring. It enables the evaluation of parameters' influence, and
867 therefore can lead to an optimization of the modeled process. Before modeling, membrane
868 ozonation was described through global mass transfer coefficients, and therefore could not be
869 scaled-up to different devices or experimental conditions. (Kukuzaki et al., 2010; Stylianou et
870 al., 2016). In addition, modelling can be used in design and optimization of cross-flow
871 membrane modules for multi-components membrane gas absorption processes.

872 Several types of computational approaches can be seen for ozone transport simulation in
873 membrane contactor processes. Three methods will be presented here. In the first one,
874 dimensionless numbers are used (in particular the Sherwood number) and hypotheses are
875 assumed in order to simplify the equations and to avoid a numerical resolution. In the second
876 approach presented here, ozone concentrations are obtained from the partial pressures. In the

last method, software like Comsol Multiphysics for example is used in order to solve the transfer equations and directly determine concentration profiles, by simulating the ozone mass transfer through a membrane into a liquid. A synthesis of several studies on this subject is available in Table 5.

Table 5: Synthesis of the studies about modelling of ozone diffusion with membrane contactors

Publication	Modeling and determination of	Type of membrane	Investigated parameters
Ozone Mass Transfer Studies in a Hydrophobized Ceramic Membrane Contactor: Experiments and Analysis. (Stylianou et al., 2016)	Concentration of dissolved ozone at the module output	Tubular membrane Porous (Ceramic - Al_2O_3)	Liquid velocity Liquid pH Gas concentration Membrane length Temperature Order of the ozone decomposition reaction
Mass transfer studies in flat-sheet membrane contactor with ozonation (Phattaranawik et al., 2005)	Ozone transfer coefficient (developed indirectly from the oxygen transport) Ozone flux Ozone concentration at membrane/liquid interface	Plane membrane Porous (PVDF)	Flow rates Temperature Matrix for ozone flux determination (pure water/solution of sodium nitrite)
A single tube contactor for testing membrane ozonation (Zoumpouli et al., 2018)	Concentration profiles Transfer resistance Transfer coefficients Ozone flux Residual ozone concentration	Tubular membrane Non porous (PDMS)	Liquid velocity Matrix (pure water/surface water/waste water/solution with humic acid) Membrane diameter Gas concentration
Modeling of ozone mass transfer through non-porous membranes for water treatment (Berry et al., 2017)	Concentration profiles Transfer resistance Overall transfer coefficient	Non porous capillary membrane (PDMS)	Membrane length, Thickness membrane Liquid velocity Gas diffusivity in the membrane Gas solubility in the membrane

6.1. Development of a mass transfer model based on dimensionless numbers

Stylianou, Kostoglou, and Zouboulis studied the ozone mass transfer in a hydrophobized ceramic membrane contactor (Stylianou et al., 2016). The gas was a mixture of ozone and oxygen, and flowed in the shell of the contactor. The liquid was in the tube. Based on experiments, the authors developed a mathematical model, representing the occurring phenomena and extracting the most important parameters. A first step was to model only the

mass transfer, without taking into account the enhancement factor due to ozone decomposition. The transfer was considered as a multiphase system with three steps: diffusion in gas phase, transfer through the membrane pores, and diffusion to water. This is therefore a convection-diffusion mechanism. Generally, the steady state partial differential conservation equation is solved in order to obtain the ozone mass transfer. However, the authors used the Leveque solution and the corresponding Sherwood number, since all the experimental conditions matched (e.g. laminar flow). The dissolved ozone concentration at the outlet of the contactor was then obtained thanks to a mass balance and the Sherwood number.

$$C_f = C_{eq} + (C_0 - C_{eq}) e^{-4LD_{O3,L}Sh / u_{L,mean} d_i^2} \quad [14]$$

With:

- C_f : Solute concentration at the tube outlet (mol.m^{-3})
- C_{eq}: Solubility of ozone in the liquid ($C_{eq} = HP_f$, where H is a variant of the Henry's law constant in mol.m^{-3}.hPa^{-1} and P_f the partial ozone pressure in hPa) (mol.m^{-3})
- C_0 : Feed ozone concentration (mol.m^{-3})
- L : Total tube length (m)
- $D_{O3,L}$: Diffusivity of ozone in the liquid phase (i.e. water) (m².s^{-1})
- Sh : Sherwood number of the liquid phase (Sh can be described by a global form such as $Sh = \frac{K_L L_c}{D} = A \times Re^B \times Sc^C$, where A, B, C are empirical constants, Sc is the Schmidt number, Re is the Reynolds number, Lc is the hydraulic diameter of the liquid phase, D is the diffusivity, and K_L is the overall mass transfer)
- $u_{L,mean}$: Mean liquid velocity (m.s^{-1})
- d_i : Internal diameter of the tube (m)

912 Then, the mass transfer model was completed with the ozone decomposition (i.e. a mass
913 transfer and reaction model were defined). Generally, conservation equations (i.e. diffusion
914 and convection terms), and reaction terms, are solved numerically. Transfer and reaction are
915 assumed to occur simultaneously. Transfer, as mentioned before, is assumed to follow
916 Leveque relation, and reaction rate is assumed to depend on the cross-sectional averaged
917 solute concentration. The governing equation for the perimeter averaged ozone concentration
918 is described by the following equation:

919 $$u_{L,mean}\frac{dC}{dz} = \frac{4DSh}{d^2}\left(C_{eq} - C\right) - r_M \quad [15]$$

920 By using the Euler explicit numerical discretization scheme with a fine mesh, for example
921 with a discretization at N points with step such as δ=L/N, a set of differential equations results
922 can be found easily.

923 For Reynolds numbers of the liquid side up to 100 (i.e. laminar regime), dissolved ozone
924 concentration at the outlet of the membrane contactor calculated with the developed model fit
925 well with the experimental results (deviation around 5%). Moreover, ozone properties (e.g.
926 diffusivity, ozone equilibrium concentration, ozone self-decomposition order and rate)
927 calculated from the model fit the experimental and theoretical data. The extrapolation of data
928 for the study of different devices and experimental conditions is possible, by changing the
929 value of major physical parameters (e.g. diffusivity, solubility). The authors also studied the
930 influence of several parameters such as the liquid velocity, the pH, the gas concentration, the
931 membrane length, and the temperature. They came to the conclusion that the pH and the
932 ozone concentration have the greatest impact on the dissolved ozone concentration at the
933 outlet of the contactor. Moreover, they noted that the ozone flux increased with the liquid
934 velocity (i.e. with the Reynolds number).

6.2. Development of a mass transfer model by using transfer coefficient and partial pressures

The mass transport in a membrane contactor (i.e. across concentration boundary layer of gas phase, through porous membrane, and liquid boundary layer) can be described with global and individual mass transfer coefficients. In order to determine these coefficients, the resistance-in-series model can be used. Phattaranawik, Leiknes, and Pronks studied ozone mass transfer in porous flat-sheet membrane contactor, made with PVDF (Phattaranawik et al., 2005). The liquid side Reynolds numbers ranged from 454 to 1469 for the experiments with O_2, and to 1136 for the experiments with O_3, both corresponding to a laminar flow. To model mass transfer without reaction, the authors determined ozone mass transfer coefficients indirectly from oxygen transfer measurements to remove ozone decomposition and potential reactions in the liquid. The oxygen mass transfer coefficient in the liquid phase is correlated to Sherwood number and can be deducted from this correlation. It can also be calculated from the Wilson plot method, a method which is also valid for the determination of the membrane mass transfer coefficient. With this method, the liquid mass transfer and the membrane mass transfer coefficients can be separated from the overall mass transfer coefficient. The authors focused on liquid mass transfer coefficient. They deduced this coefficient for the ozone from the oxygen coefficient, using in particular the surface renewal theory (see Equation 15).

$$k_{L,O3} = \left(\frac{D_{O3,L}}{D_{O2,L}}\right)^{0.5} \times k_{L,O2} = 0.789 \times k_{L,O2} \quad \text{(Cussler, 2009)} \quad [15]$$

To model ozone mass transfer with a chemical reaction, an enhancement factor was added to the individual transfer coefficient of the liquid film. The global transfer coefficient is described by the equation [12] (see 3.2.4. The overall mass transfer coefficient).

957 The authors described the procedure followed for calculating ozone fluxes without chemical
958 reaction (i.e. with pure water), and with chemical reaction (i.e. with sodium nitrite solutions).
959 The procedure with pure water can be summarized in several main steps. First, the ozone flux
960 is assumed and the effluent ozone concentrations in both gas and liquid streams are calculated
961 by mass balance. The average ozone concentrations are then determined. The concentrations
962 at both membrane surfaces, and the ozone partial pressures at the membrane surfaces are
963 calculated, and the flux are deducted from these pressures. Finally, the new calculated flux is
964 compared with the flux previously assumed. When the difference between the assumed and
965 the calculated flux is smaller than 0.01%, the procedure is finished. If not, the calculated flux
966 is the new assumed flux, and the procedure begins again (i.e. the loop begins again). With a
967 chemical reactions, the procedure is more complex than without, due to the presence of
968 oxidation. Phattaranawik at al. concluded that both procedures can be used to design the
969 ozonation membrane contactor in pilot scale. However, the mathematical model should be
970 refined with residual ozone concentration because of the authors' assumption of zero effluent
971 ozone concentrations in the liquid stream.

972 ### 6.3. Determination of concentration profiles with software for the resolution of transfer
973 equations

974 Another approach is the numerical modeling thanks to Computational Fluid Dynamics
975 (CFD) software (Berry et al., 2017; Zoumpouli et al., 2018). The steps of the CFD
976 simulation set-up are described by Tu et al. (Tu et al., 2018). The first step is to define a
977 domain (2-D or 3-D) and a geometry based on the studied membrane dimensions. For a
978 gas/liquid membrane contactor, 3 domains can be defined: the gas phase, the membrane,
979 the liquid phase. Then, the optimal mesh has to be chosen in order to obtain the best
980 compromise between accuracy and computing time. The model can be scaled if necessary,
981 and the convergence criteria have to be set, representing the acceptable residual after all the

iterations. The next step is the specification of the governing equations (i.e. species and momentum equations), and of the boundary conditions. The CFD software takes care to couple and solve these equations, and therefore concentration profiles are obtained (Berry et al., 2017) .

During their works, Berry et al. used Comsol Multiphysics ® in order to obtain concentration profiles. The simulation was made with the gas flowing inside the tube and the liquid outside, in a non-porous capillary membrane made with PDMS. The gas was pure oxygen or a mixture of ozone and oxygen. Variations from 3.5 to 2210 of the liquid side Reynolds number were performed, corresponding to a laminar flow. The regime was also laminar on the gas side. The equations solved by the software, and their application conditions, are synthetized in Table 6.

Table 6: Governing equations of the mass transport used by Berry et al.

		Gas section ($0 \leq r \leq Ri$)	Membrane section ($0 \leq r \leq Ri+Lm$)	Liquid section ($Ri+Lm \leq r \leq Ri+Lm+Lw$)
Momentum transport	Assumptions	Ideal and incompressible gas Laminar, steady state, and Newtonian flow	gas velocity negligible because of the low gas permeability in the membranes	Laminar, steady, and fully developped flow Co-current configuration. Constant liquid density and constant liquid viscosity.
	Boundary conditions	axial symetrie : no flow crossing the boudary ($u_{r,g}= 0$ when $r=0$) membrane wall: no-slip ($u_{z,g}=0$ whan $r=Ri$) the velocity in the r-directions at all the boundaries are almost zero ($u_{r,g}=0$)	x	Velocity in the r-directions at all the boundaries almost null ($u_{r,L}= 0$) Membrane wall : no-slip ($u_{z,L}= 0$ when $r=Ri+Lm$) Inlet: Averaged velocity specified at the inlet ($u_{z,L}=u_{L,mean}$ whenz=0)

		Tube inlet: flow is fully developped and velocituy profile is parabolic ($u_{z,g}=2u_{g,mean}[1-(r/Ri)^2]$) Tube outlet: flow is fully developped ($\partial u_{z,g}/\partial z=0$ when z=0)		Outlet: Fully developped flow ($\partial u_{z,L}/\partial z=0$ when z=L)
	Equations	Continuity: $\nabla . u_g$ Navier-Stokes: $\rho_g(u_g . \nabla u_g) = -\nabla \rho_g + \mu_g \nabla^2 u_g$	ug=0	Continuity: $\nabla . u_L$ Navier-Stokes: $\rho_L(u_L . \nabla u_L) = -\nabla \rho_L + \mu_L \nabla^2 u_L$
Species transport	Assumptions	Transport only by diffusion and convection, no reaction taking place in the system	Transport only by diffusion and convection, no reaction taking place in the system. No mutual interaction between the gases of the mixture (O_2/O_3) (Dhingra and Marand, 1998)	Isotropic mass diffusivity of i
	Boundary conditions	Axial symmetry: no material flow across the boundary ($\partial u_{g,j}/\partial r=0$ when r=0) Tube inlet: $C_{g,j}=C_{g,j,0}$ Tube outlet: the gas flux is predominantly by convection ($\partial u_{g,j}/\partial z=0$ when z=L)	Gas-membrane interface: interfacial transport defined by the solubility laws ($C_{m1,j}=C_{g,j,i}/S_j$ when r=Ri) Membrane inlet: insulated boundary ($\partial C_{m,j}/\partial z=0$ when z=0) Membrane outlet: insulated boundary ($\partial C_{m,j}/\partial z=0$ when z=L)	Concentrations of O_2 and O_3 nulle: $C_{L,j,0}=0$ Membrane-liquid interface: interfacial transport defined by the solubility laws ($C_{m1,j}=H_j C_{L,j,i}$ when r=Ri+Lm)
	Equations	$u_g . \nabla C_{g,j} = D_{g,j} \nabla^2 C_{g,j}$	$D_{m,j}\left[\frac{1}{r}\frac{\partial\left(r\frac{\partial C_{m,j}}{\partial x}\right)}{\partial r} + \frac{\partial^2 C_{m,j}}{\partial z^2}\right] = 0$	$u_L . \nabla C_{L,j} = x\nabla^2 C_{L,j}$

The model established by the authors resulted in the determination of the concentration profiles. It can be used as a base for the prediction of the ozone and oxygen transfer for various designs, materials, and hydraulic conditions. Sherwood numbers obtained with this model fit with those found in the literature (Berry et al., 2017) . The main conclusions are as follow. First, the gas solubility is a parameter which cannot be neglected, in particular for the oxygen. The main resistance of the ozone transfer is on the liquid side, and the main resistance of the oxygen transfer is in the membrane.

Zoumpouli et al. had a similar approach than Berry et al. (Zoumpouli et al., 2018). However, the configuration of the membrane contactor was different. The simulation was made with the

liquid flowing inside the tube and the gas in the shell, in a non-porous tubular membrane made with PDMS. The gas studied was a mixture of ozone and oxygen. The effect of added peroxone (i.e. H_2O_2) in the liquid phase was also investigated. The liquid side Reynolds number was varied up to 290. For Reynolds numbers less than 100, the simulation results were moderately overpredicted, in comparison to experimental measures. This may be a result of a non-uniform dispersion of O_3 for low flowrates. For Reynolds numbers over 100, results obtained during the experiments fitted well with the simulation results, with an absolute difference lower than 0,5 mg/L. Their main conclusion is the importance of the liquid velocity as a major parameter for the determination of the ozone global transfer, followed, in that order, by the membrane length and the gas concentration.

7. Conclusion

Membrane contactors for ozone diffusion is a recent unit operation for water treatment by ozonation. Using a hollow fiber membrane contactor, ozone is added uniformly to the water to be treated, through many dosing points and with a great mass transfer surface area. It leads to a better transformation rate of micropollutants than with conventional ozonation processes, and potentially to a lower bromates' formation thanks to a lower residual ozone concentration.

In addition, membrane contactors offer other advantages, like its modularity, its small foot print, and the independent flow adjustment for gas and liquid phases. Gas can also be recycled, leading to energy and reagents savings.

Many parameters influence the mass transfer during ozonation using membrane contactors. When carefully chosen, the efficiency of the process can then be greatly enhanced. For instance, the choice of the fiber material used is a crucial parameter. It has to provide a good ozone transfer through the membrane, but resist to ozone even for a long use. PTFE and PVDF membranes seem to be good choices for an ozonation application. The pressures to

apply to the different phases also depend on the material chosen. The transmembrane pressure seems to be the major difficulty of membrane contactor technology. It has to be set carefully, in order to avoid bubbling and wetting problems.

The modeling of membrane processes for ozonation is useful to optimize reactor design and operating conditions and to study the influence of membrane properties. This optimization enables to achieve the best pollutant removal, for the minimum by-products' production and the minimum ozone consumption.

. An important challenge to overcome will be the development of more efficient membrane material. Hydrophobic membranes have to be manufactured with coating or grafting techniques, which could lead to complicated modification routes and excessive use of chemicals. Moreover, studies about long term stability of the membranes used will be essential to apply the process on an industrial scale. Finally, a key point concerns the manufacture of affordable module with an optimized hydrodynamic and a high mass transfer coefficient.

Bibliography

Ahmed, T., Semmens, M.J., 1992a. The use of independently sealed microporous hollow fiber membranes for oxygenation of water: model development. J. Memb. Sci. 69, 11–20.

Ahmed, T., Semmens, M.J., 1992b. Use of sealed end hollow fibers for bubbleless membrane aeration: experimental studies. J. Memb. Sci. 69, 1–10.

Ahmed, T., Semmens, M.J., Voss, M.A., 2004. Oxygen transfer characteristics of hollow-fiber, composite membranes. Adv. Environ. Res. 8, 637–646.

AIDA, 1998. Directive n° 98/83/CE du 03/11/98 relative à la qualité des eaux destinées à la

consommation humaine.

Al-Saffar, H.B., Oklany, J.S., Ozturk, B., Hughes, R., 1995. Removal of carbon dioxide from gas streams using a gas/liquid hollow fibre module. Process Saf. Environ. Prot. 73, 144–150.

Alves dos Santos, F.R., Borges, C.P., da Fonseca, F.V., 2015. Polymeric Materials for Membrane Contactor Devices Applied to Water Treatment by Ozonation. Mater. Res. 18, 1015–1022. https://doi.org/10.1590/1516-1439.016715

Amin, S.K., Abdallah, H.A.M., Roushdy, M.H., El-Sherbiny, S.A., 2016. An overview of production and development of ceramic membranes. Int. J. Appl. Eng. Res. 11, 7708–7721.

Antoniou, M.G., Hey, G., Rodríguez Vega, S., Spiliotopoulou, A., Fick, J., Tysklind, M., la Cour Jansen, J., Andersen, H.R., 2013. Required ozone doses for removing pharmaceuticals from wastewater effluents. Sci. Total Environ. 456–457, 42–49. https://doi.org/10.1016/j.scitotenv.2013.03.072

Atchariyawut, S., Jiraratananon, R., Wang, R., 2007. Separation of CO2 from CH4 by using gas–liquid membrane contacting process. J. Memb. Sci. 304, 163–172. https://doi.org/10.1016/j.memsci.2007.07.030

Atchariyawut, S., Phattaranawik, J., Leiknes, T., Jiraratananon, R., 2009. Application of ozonation membrane contacting system for dye wastewater treatment. Sep. Purif. Technol. 66, 153–158. https://doi.org/10.1016/j.seppur.2008.11.011

Bakeri, G., Matsuura, T., Ismail, A.F., Rana, D., 2012. A novel surface modified polyetherimide hollow fiber membrane for gas–liquid contacting processes. Sep. Purif. Technol. 89, 160–170. https://doi.org/10.1016/J.SEPPUR.2012.01.022

1076 Bamperng, S., Suwannachart, T., Atchariyawut, S., Jiraratananon, R., 2010. Ozonation of dye
1077 wastewater by membrane contactor using PVDF and PTFE membranes. Sep. Purif.
1078 Technol. 72, 186–193. https://doi.org/10.1016/j.seppur.2010.02.006

1079 Bauer, W.G., Fredrickson, A.G., Tsuchiya, H.M., 1963. Mass transfer characteristics of a
1080 venturi liquid-gas contactor. Ind. Eng. Chem. Process Des. Dev. 2, 178–187.
1081 https://doi.org/10.1021/i260007a002

1082 Behera, S.K., Kim, H.W., Oh, J.-E., Park, H.-S., 2011. Occurrence and removal of antibiotics,
1083 hormones and several other pharmaceuticals in wastewater treatment plants of the largest
1084 industrial city of Korea. Sci. Total Environ. 409, 4351–4360.
1085 https://doi.org/10.1016/J.SCITOTENV.2011.07.015

1086 Berry, M.J., Taylor, C.M., King, W., Chew, Y.M.J., Wenk, J., 2017. Modelling of Ozone
1087 Mass-Transfer through Non-Porous Membranes for Water Treatment. Water 9, 452.
1088 https://doi.org/10.3390/w9070452

1089 Boon, A.G., 1980. Measurement of aerator performance, in: Papers Presented at the
1090 Symposium on the Profitable Aeration of Waste Water, Held at the Sudbury Conference
1091 Hall, London, April 1980/Organized and Sponsored by BHRA Fluid Engineering.
1092 Cranfield, Eng.: BHRA Fluid Engineering, c1980.

1093 Boucif, N., 2012. Modélisation et simulation de contacteurs membranaires pour les procédés
1094 d'absorption de gaz acides par solvant chimique. Lorraine, Nancy.

1095 Bourgin, M., Borowska, E., Helbing, J., Hollender, J., Kaiser, H.-P., Kienle, C., McArdell,
1096 C.S., Simon, E., von Gunten, U., 2017. Effect of operational and water quality
1097 parameters on conventional ozonation and the advanced oxidation process O3/H2O2:
1098 Kinetics of micropollutant abatement, transformation product and bromate formation in a

surface water. Water Res. 122, 234–245. https://doi.org/10.1016/j.watres.2017.05.018

Briens, C.L., Huynh, L.X., Large, J.F., Catros, A., Bernard, J.R., Bergougnou, M.A., 1992. Hydrodynamics and gas-liquid mass transfer in a downward venturi-bubble column combination. Chem. Eng. Sci. 47, 3549–3556. https://doi.org/10.1016/0009-2509(92)85069-N

Buffle, M.O., Schumacher, J., Meylan, S., Jekel, M., Von Gunten, U., 2006. Ozonation and advanced oxidation of wastewater: Effect of O3 dose, pH, DOM and HO.-scavengers on ozone decomposition and HO . generation. Ozone Sci. Eng. 28, 247–259. https://doi.org/10.1080/01919510600718825

Cachon, R., Girardon, P., Voilley, A., 2019. Gases in Agro-food Processes.

Chabanon, E., Favre, E., 2017. 3.9 Membranes Contactors for Intensified Gas–Liquid Absorption Processes. Compr. Membr. Sci. Eng. https://doi.org/10.1016/B978-0-12-409547-2.12250-4

Choi, Y.J., Kim, M., 2011. Preparation and characterization of polyvinylidene fluoride by irradiating electron beam. Appl. Chem. Eng. 22, 353–357. https://doi.org/10.1021/ie010553y

Ciora, R.J., Liu, P.K.T., 2003. Ceramic membranes for environmental related applications. Fluid - Part. Sep. J. 15, 51–60.

Côté, P., Bersillon, J.-L., Huyard, A., 1989. Bubble-free aeration using membranes: mass transfer analysis. J. Memb. Sci. 47, 91–106. https://doi.org/https://doi.org/10.1016/S0376-7388(00)80862-5

Cruz-Alcalde, A., Esplugas, S., Sans, C., 2019. Abatement of ozone-recalcitrant

micropollutants during municipal wastewater ozonation: Kinetic modelling and surrogate-based control strategies. Chem. Eng. J. 360, 1092–1100. https://doi.org/10.1016/j.cej.2018.10.206

Cussler, E.L., 2009. Diffusion : mass transfer in fluid systems. Cambridge University Press.

deMontigny, D., Tontiwachwuthikul, P., Chakma, A., 2006. Using polypropylene and polytetrafluoroethylene membranes in a membrane contactor for CO2 absorption. J. Memb. Sci. 277, 99–107. https://doi.org/https://doi.org/10.1016/j.memsci.2005.10.024

Dhingra, S.S., Marand, E., 1998. Mixed gas transport study through polymeric membranes. J. Memb. Sci. 141, 45–63. https://doi.org/10.1016/S0376-7388(97)00285-8

Dindore, V.Y., Brilman, D.W.F., Versteeg, G.F., 2005. Modelling of cross-flow membrane contactors: Physical mass transfer processes. J. Memb. Sci. 251, 209–222. https://doi.org/10.1016/j.memsci.2004.11.017

Drioli, E., Criscuoli, A., Curcio, E., 2006. Membrane contactors : fundamentals, applications and potentialities. Elsevier.

Elovitz, M.S., Von Gunten, U., 1999. Hydroxyl Radical/Ozone Ratios During Ozonation Processes. I. The Rct Concept. Ozone Sci. Eng. J. Int. Ozone Assoc. 21, 239–260. https://doi.org/10.1080/01919519908547239

Elovitz, M.S., Von Gunten, U., Kaiser, H.-P., 2000. Hydroxyl Radical/Ozone Ratios During Ozonation Processes. II. The Effect of Temperature, pH, Alkalinity, and DOM Properties. Ozone Sci. Eng. J. Int. Ozone Assoc. 22, 123–150. https://doi.org/10.1080/01919510008547216

Faiz, R., Fallanza, M., Ortiz, I., Li, K., 2013. Separation of olefin/paraffin gas mixtures using

1143 ceramic hollow fiber membrane contactors. Ind. Eng. Chem. Res. 52, 7918–7929.
1144 https://doi.org/10.1021/ie400870n

1145 Fang, Y., Novak, P.J., Hozalski, R.M., Cussler, E.L., Semmens, M.J., 2004. Condensation
1146 studies in gas permeable membranes. J. Memb. Sci. 231, 47–55.
1147 https://doi.org/https://doi.org/10.1016/j.memsci.2003.10.039

1148 Gabelman, A., Hwang, S.T., 1999. Hollow fiber membrane contactors. J. Memb. Sci. 159,
1149 61–106. https://doi.org/10.1016/S0376-7388(99)00040-X

1150 Gao, Y., Ji, Y., Li, G., An, T., 2016. Theoretical investigation on the kinetics and mechanisms
1151 of hydroxyl radical-induced transformation of parabens and its consequences for
1152 toxicity: Influence of alkyl-chain length. Water Res. 91, 77–85.
1153 https://doi.org/10.1016/j.watres.2015.12.056

1154 Gogoi, A., Mazumder, P., Tyagi, V.K., Tushara Chaminda, G.G., An, A.K., Kumar, M., 2018.
1155 Occurrence and fate of emerging contaminants in water environment: A review.
1156 Groundw. Sustain. Dev. 6, 169–180. https://doi.org/10.1016/j.gsd.2017.12.009

1157 Goh, P.S., Naim, R., Rahbari-Sisakht, M., Ismail, A.F., 2019. Modification of membrane
1158 hydrophobicity in membrane contactors for environmental remediation. Sep. Purif.
1159 Technol. 227, 115721. https://doi.org/10.1016/J.SEPPUR.2019.115721

1160 Gomes, J., Costa, R., Quinta-Ferreira, R.M., Martins, R.C., 2017. Application of ozonation
1161 for pharmaceuticals and personal care products removal from water. Sci. Total Environ.
1162 586, 265–283. https://doi.org/10.1016/j.scitotenv.2017.01.216

1163 Gordon, G., 1995. The chemistry and reactions of ozone in our environment. Prog. Nucl.
1164 Energy 29, 89–96. https://doi.org/10.1016/0149-1970(95)00031-E

1165 Guerra, K., Pellegrino, J., 2013. Development of a Techno-Economic Model to Compare
1166 Ceramic and Polymeric Membranes. Sep. Sci. Technol. 48, 51–65.
1167 https://doi.org/10.1080/01496395.2012.690808

1168 Guo, Y., Wang, H., Wang, B., Deng, S., Huang, J., Yu, G., Wang, Y., 2018. Prediction of
1169 micropollutant abatement during homogeneous catalytic ozonation by a chemical kinetic
1170 model. Water Res. 142, 383–395. https://doi.org/10.1016/j.watres.2018.06.019

1171 Hansen, K.M.S., Spiliotopoulou, A., Chhetri, R.K., Escolà Casas, M., Bester, K., Andersen,
1172 H.R., 2016. Ozonation for source treatment of pharmaceuticals in hospital wastewater –
1173 Ozone lifetime and required ozone dose. Chem. Eng. J. 290, 507–514.
1174 https://doi.org/10.1016/j.cej.2016.01.027

1175 Heeb, M.B., Criquet, J., Zimmermann-Steffens, S.G., Von Gunten, U., 2014. Oxidative
1176 treatment of bromide-containing waters: Formation of bromine and its reactions with
1177 inorganic and organic compounds - A critical review. Water Res. 48, 15–42.
1178 https://doi.org/10.1016/j.watres.2013.08.030

1179 Hollender, J., Zimmermann, S.G., Koepke, S., Krauss, M., McArdell, C.S., Ort, C., Singer,
1180 H., von Gunten, U., Siegrist, H., 2009. Elimination of organic micropollutants in a
1181 municipal wastewater treatment plant upgraded with a full-scale post-ozonation followed
1182 by sand filtration. Environ. Sci. Technol. 43, 7862–7869.
1183 https://doi.org/10.1021/es9014629

1184 Huber, M.M., Canonica, S., Park, G.-Y., von Gunten, U., 2003. Oxidation of Pharmaceuticals
1185 during Ozonation and Advanced Oxidation Processes. Environ. Sci. Technol. 37, 1016–
1186 1024. https://doi.org/10.1021/es025896h

1187 Janknecht, P., Wilderer, P.A., Picard, C., Larbot, A., 2001. Ozone–water contacting by

ceramic membranes. Sep. Purif. Technol. 25, 341–346. https://doi.org/https://doi.org/10.1016/S1383-5866(01)00061-2

Jansen, R.H.S., de Rijk, J.W., Zwijnenburg, A., Mulder, M.H.V., Wessling, M., 2005. Hollow fiber membrane contactors—A means to study the reaction kinetics of humic substance ozonation. J. Memb. Sci. 257, 48–59. https://doi.org/10.1016/J.MEMSCI.2004.07.038

Kanakaraju, D., Glass, B.D., Oelgemoller, M., 2018. Advanced oxidation process-mediated removal of pharmaceuticals from water: A review. J. Environ. Manage. 219, 189–207. https://doi.org/10.1016/j.jenvman.2018.04.103

Khaisri, S., deMontigny, D., Tontiwachwuthikul, P., Jiraratananon, R., 2009. Comparing membrane resistance and absorption performance of three different membranes in a gas absorption membrane contactor. Sep. Purif. Technol. 65, 290–297. https://doi.org/10.1016/j.seppur.2008.10.035

Kim, J., Davies, S.H.R., Baumann, M.J., Tarabara, V. V., Masten, S.J., 2008. Effect of ozone dosage and hydrodynamic conditions on the permeate flux in a hybrid ozonation-ceramic ultrafiltration system treating natural waters. J. Memb. Sci. 311, 165–172. https://doi.org/10.1016/j.memsci.2007.12.010

Kukuzaki, M., Fujimoto, K., Kai, S., Ohe, K., Oshima, T., Baba, Y., 2010. Ozone mass transfer in an ozone-water contacting process with Shirasu porous glass (SPG) membranes-A comparative study of hydrophilic and hydrophobic membranes. Sep. Purif. Technol. 72, 347–356. https://doi.org/10.1016/j.seppur.2010.03.004

Kwon, Y.-N., Hong, S., Choi, H., Tak, T., 2012. Surface modification of a polyamide reverse osmosis membrane for chlorine resistance improvement. J. Memb. Sci. 415–416, 192–198. https://doi.org/10.1016/J.MEMSCI.2012.04.056

1211 Kwon, Y.-N., Joksimovic, R., Kim, I.-C., Leckie, J.O., 2011. Effect of bromide on the
1212 chlorination of a polyamide membrane. Desalination 280, 80–86.
1213 https://doi.org/10.1016/J.DESAL.2011.06.046

1214 Laera, G., Cassano, D., Lopez, A., Pinto, A., Pollice, A., Ricco, G., Mascolo, G., 2012.
1215 Removal of organics and degradation products from industrial wastewater by a
1216 membrane bioreactor integrated with ozone or UV/H 2O 2 treatment. Environ. Sci.
1217 Technol. 46, 1010–1018. https://doi.org/10.1021/es202707w

1218 Lee, Y., Gerrity, D., Lee, M., Bogeat, A.E., Salhi, E., Gamage, S., Trenholm, R.A., Wert,
1219 E.C., Snyder, S.A., von Gunten, U., 2013. Prediction of micropollutant elimination
1220 during ozonation of municipal wastewater effluents: use of kinetic and water specific
1221 information. Environ. Sci. Technol. 47, 5872–5881. https://doi.org/10.1021/es400781r

1222 Lee, Y., Kovalova, L., McArdell, C.S., von Gunten, U., 2014. Prediction of micropollutant
1223 elimination during ozonation of a hospital wastewater effluent. Water Res. 64, 134–148.
1224 https://doi.org/10.1016/J.WATRES.2014.06.027

1225 Lee, Y., von Gunten, U., 2016. Advances in predicting organic contaminant abatement during
1226 ozonation of municipal wastewater effluent: reaction kinetics, transformation products,
1227 and changes of biological effects. Environ. Sci. Water Res. Technol. 2, 421–442.
1228 https://doi.org/10.1039/C6EW00025H

1229 Leiknes, T., Phattaranawik, J., Boller, M., Von Gunten, U., Pronk, W., 2005. Ozone transfer
1230 and design concepts for NOM decolourization in tubular membrane contactor. Chem.
1231 Eng. J. 111, 53–61. https://doi.org/10.1016/j.cej.2005.05.007

1232 Li, J., Zhu, L.-P., Xu, Y.-Y., Zhu, B.-K., 2010. Oxygen transfer characteristics of hydrophilic
1233 treated polypropylene hollow fiber membranes for bubbleless aeration. J. Memb. Sci.

362, 47–57. https://doi.org/https://doi.org/10.1016/j.memsci.2010.06.013

Lishman, L., Smyth, S.A., Sarafin, K., Kleywegt, S., Toito, J., Peart, T., Lee, B., Servos, M., Beland, M., Seto, P., 2006. Occurrence and reductions of pharmaceuticals and personal care products and estrogens by municipal wastewater treatment plants in Ontario, Canada. Sci. Total Environ. 367, 544–558.

Luo, Y., Guo, W., Ngo, H.H., Nghiem, L.D., Hai, F.I., Zhang, J., Liang, S., Wang, X.C., 2014. A review on the occurrence of micropollutants in the aquatic environment and their fate and removal during wastewater treatment. Sci. Total Environ. 473–474, 619–641. https://doi.org/10.1016/j.scitotenv.2013.12.065

Margot, J., Kienle, C., Magnet, A., Weil, M., Rossi, L., de Alencastro, L.F., Abegglen, C., Thonney, D., Chèvre, N., Schärer, M., Barry, D.A., 2013. Treatment of micropollutants in municipal wastewater: Ozone or powdered activated carbon? Sci. Total Environ. 461–462, 480–498. https://doi.org/10.1016/j.scitotenv.2013.05.034

Mark, J.E., 1999. Polymer Data Handbook. OXFORD UNIVERSITY PRESS.

Mavroudi, M., Kaldis, S.P., Sakellaropoulos, G.P., 2006. A study of mass transfer resistance in membrane gas–liquid contacting processes. J. Memb. Sci. 272, 103–115. https://doi.org/10.1016/J.MEMSCI.2005.07.025

Mecha, A.C., Onyango, M.S., Ochieng, A., Momba, M.N.B., 2016. Impact of ozonation in removing organic micro-pollutants in primary and secondary municipal wastewater: Effect of process parameters. Water Sci. Technol. 74, 756–765. https://doi.org/10.2166/wst.2016.276

Merle, T., Pronk, W., Von Gunten, U., Eawag, †, 2017. MEMBRO 3 X, a Novel Combination of a Membrane Contactor with Advanced Oxidation (O 3 /H 2 O 2) for Simultaneous

1257 Micropollutant Abatement and Bromate Minimization. Environ. Sci. Technol. Lett 4, 13.
1258 https://doi.org/10.1021/acs.estlett.7b00061

1259 Mori, Y., Oota, T., Hashino, M., Takamura, M., Fujii, Y., 1998. Ozone-microfiltration
1260 system. Desalination 117, 211–218. https://doi.org/10.1016/S0011-9164(98)00098-8

1261 Mulder, M., 1996. Basic principles of membrane technology, 2nd ed. ed. Kluwer Academic,
1262 Dordrecht ; Boston.

1263 Nakada, N., Shinohara, H., Murata, A., Kiri, K., Managaki, S., Sato, N., Takada, H., 2007.
1264 Removal of selected pharmaceuticals and personal care products (PPCPs) and endocrine-
1265 disrupting chemicals (EDCs) during sand filtration and ozonation at a municipal sewage
1266 treatment plant. Water Res. 41, 4373–4382.
1267 https://doi.org/10.1016/J.WATRES.2007.06.038

1268 Nawrocki, J., Kasprzyk-Hordern, B., 2010. The efficiency and mechanisms of catalytic
1269 ozonation. Appl. Catal. B Environ. 99, 27–42.
1270 https://doi.org/10.1016/j.apcatb.2010.06.033

1271 Nguyen, P.T., 2018. Contacteurs à membranes denses pour les procédés d ’ absorption gaz-
1272 liquide intensifiés : application à la capture du CO 2 en post combustion Phuc Tien
1273 Nguyen To cite this version : HAL Id : tel-01748894 soutenance et mis à disposition de l
1274 ’ ensemble de .

1275 Nguyen, P.T., Lasseuguette, E., Medina-Gonzalez, Y., Remigy, J.C., Roizard, D., Favre, E.,
1276 2011. A dense membrane contactor for intensified CO2 gas/liquid absorption in post-
1277 combustion capture. J. Memb. Sci. 377, 261–272.
1278 https://doi.org/10.1016/J.MEMSCI.2011.05.003

1279 Nobukawa, T., Sanukida, S., 2000. The genotoxity of by-products by chlorination and

ozonation of the river water in the presence of bromide ions. Water Sci. Technol. 42, 259–264. https://doi.org/10.2166/wst.2000.0389

Office fédéral de l'environnement, D.E., 2014. Rapport explicatif concernant la modification de l'ordonnance sur la protection des eaux.

Ozkan, F., Ozturk, M., Baylar, A., 2006. Experimental investigations of air and liquid injection by venturi tubes. Water Environ. J. 20, 114–122. https://doi.org/10.1111/j.1747-6593.2005.00003.x

Pabby, A.K., Sastre, A.M., 2013. State-of-the-art review on hollow fibre contactor technology and membrane-based extraction processes. J. Memb. Sci. 430, 263–303. https://doi.org/10.1016/j.memsci.2012.11.060

Paxéus, N., 2004. Removal of selected non-steroidal anti-inflammatory drugs (NSAIDs), gemfibrozil, carbamazepine, b-blockers, trimethoprim and triclosan in conventional wastewater treatment plants in five EU countries and their discharge to the aquatic environment. Water Sci. Technol. 50, 253–260. https://doi.org/10.2166/wst.2004.0335

Petala, M., Samaras, P., Zouboulis, A., Kungolos, A., Sakellaropoulos, G.P.P., 2008. Influence of ozonation on the in vitro mutagenic and toxic potential of secondary effluents. Water Res. 42, 4929–4940. https://doi.org/10.1016/J.WATRES.2008.09.018

Petala, M., Tsiridis, V., Samaras, P., Zouboulis, A., Sakellaropoulos, G.P.P., 2006. Wastewater reclamation by advanced treatment of secondary effluents. Desalination 195, 109–118. https://doi.org/10.1016/J.DESAL.2005.10.037

Phattaranawik, J., Leiknes, T., Pronk, W., 2005. Mass transfer studies in flat-sheet membrane contactor with ozonation. J. Memb. Sci. 247, 153–167. https://doi.org/10.1016/j.memsci.2004.08.020

1303 Picard, C., Larbot, A., Sarrazin, J., Janknecht, P., Wilderer, P., 2001. Ceramic membranes for
1304 ozonation in wastewater treatment. Ann. Chim. - Sci. des Matériaux 26, 13–22.
1305 https://doi.org/10.1016/S0151-9107(01)80042-8

1306 Pines, D., Min, K.-N., J. Ergas, S., Reckhow, D., 2005. Investigation of an Ozone Membrane
1307 Contactor System. https://doi.org/10.1080/01919510590945750

1308 Prieto-Rodríguez, L., Oller, I., Klamerth, N., Agüera, A., Rodríguez, E.M., Malato, S., 2013.
1309 Application of solar AOPs and ozonation for elimination of micropollutants in municipal
1310 wastewater treatment plant effluents. Water Res. 47, 1521–1528.
1311 https://doi.org/10.1016/j.watres.2012.11.002

1312 Reed, B.W., Semmens, M.J., Cussler, E.L., 1995. Chapter 10 Membrane contactors. Membr.
1313 Sci. Technol. 2, 467–498. https://doi.org/10.1016/S0927-5193(06)80012-4

1314 Reungoat, J., Escher, B.I.I., Macova, M., Argaud, F.X.X., Gernjak, W., Keller, J., 2012.
1315 Ozonation and biological activated carbon filtration of wastewater treatment plant
1316 effluents. Water Res. 46, 863–872. https://doi.org/10.1016/J.WATRES.2011.11.064

1317 Reungoat, J., Macova, M., Escher, B.I.I., Carswell, S., Mueller, J.F.F., Keller, J., 2010.
1318 Removal of micropollutants and reduction of biological activity in a full scale
1319 reclamation plant using ozonation and activated carbon filtration. Water Res. 44, 625–
1320 637. https://doi.org/10.1016/J.WATRES.2009.09.048

1321 Richardson, S.D., 2003. Disinfection by-products and other emerging contaminants in
1322 drinking water. TrAC Trends Anal. Chem. 22, 666–684. https://doi.org/10.1016/S0165-
1323 9936(03)01003-3

1324 Rosal, R., Rodríguez, A., Perdigón-Melón, J.A., Petre, A., García-Calvo, E., Gómez, M.J.,
1325 Agüera, A., Fernández-Alba, A.R., 2010. Occurrence of emerging pollutants in urban

wastewater and their removal through biological treatment followed by ozonation. Water Res. 44, 578–588. https://doi.org/10.1016/J.WATRES.2009.07.004

Roustan, M., 2003. Transferts gaz-liquide dans les procédés de traitement des eaux et des effluents gazeux. Éd. Tec & doc, Paris; Londres; New York.

Roustan, M., Debellefontaine, H., Do-Quang, Z., Duguet, J.-P., 1998. Development of a Method for the Determination of Ozone Demand of a Water. Ozone Sci. Eng. 20, 513–520. https://doi.org/10.1080/01919519809480338

Samadi, M.T., Azarian, G., Seifipour, F., Huang, C.P., Yang, X., Poormohammadi, A., 2015. The formation of aldehydes and ketones ozonation by-products and their variation through general water treatment plant in hamadan, Iran. Glob. Nest J. 17, 682–691.

Santos, J.L., Aparicio, I., Alonso, E., 2007. Occurrence and risk assessment of pharmaceutically active compounds in wastewater treatment plants. A case study: Seville city (Spain). Environ. Int. 33, 596–601. https://doi.org/https://doi.org/10.1016/j.envint.2006.09.014

Schlüter-Vorberg, L., Prasse, C., Ternes, T.A., Mückter, H., Coors, A., 2015. Toxification by transformation in conventional and advanced wastewater treatment: the antiviral drug acyclovir. Environ. Sci. Technol. Lett. 2, 342–346. https://doi.org/10.1021/acs.estlett.5b00291

Schwarzenbach, R.P., Escher, B.I., Fenner, K., Hofstetter, T.B., Johnson, C.A., von Gunten, U., Wehrli, B., 2006. The Challenge of Micropollutants in Aquatic Systems. Science (80-.). 313, 1072–1077. https://doi.org/10.1126/science.1127291

Shanbhag, P.V., Guha, A.K., Sirkar, K.K., 1995. Single-phase membrane ozonation of hazardous organic compounds in aqueous streams. J. Hazard. Mater. 41, 95–104.

https://doi.org/10.1016/0304-3894(94)00097-Z

Shanbhag, P. V, Guha, A.K., Sirkar, K.K., 1998. Membrane-Based Ozonation of Organic Compounds. Ind. Eng. Chem. Res. 37, 4388–4398. https://doi.org/10.1021/ie980182u

Shen, Z., Semmens, M.J., Collins, A.G., 1990. A novel approach to ozone - water mass transfer using hollow - fiber reactors. Environ. Technol. 11, 597–608. https://doi.org/10.1080/09593339009384902

Smolders, K., Franken, A.C.M.C.M., 1989. Terminology for Membrane Distillation. Desalination 72, 249–262. https://doi.org/10.1016/0011-9164(89)80010-4

Snyder, S.A., Wert, E.C., Rexing, D.J., Zegers, R.E., Drury, D.D., 2006. Ozone oxidation of endocrine disruptors and pharmaceuticals in surface water and wastewater. Ozone Sci. Eng. 28, 445–460. https://doi.org/10.1080/01919510601039726

Sotelo, J.L., Beltrán, F.J., Benitez, F.J., Beltrán-Heredia, J., 1989. Henry's law constant for the ozone-water system. Water Res. 23, 1239–1246. https://doi.org/https://doi.org/10.1016/0043-1354(89)90186-3

Stalter, D., Magdeburg, A., Oehlmann, J., 2010a. Comparative toxicity assessment of ozone and activated carbon treated sewage effluents using an in vivo test battery. Water Res. 44, 2610–2620. https://doi.org/10.1016/J.WATRES.2010.01.023

Stalter, D., Magdeburg, A., Weil, M., Knacker, T., Oehlmann, J., 2010b. Toxication or detoxication? In vivo toxicity assessment of ozonation as advanced wastewater treatment with the rainbow trout. Water Res. 44, 439–448. https://doi.org/10.1016/J.WATRES.2009.07.025

Stylianou, S.K., Katsoyiannis, I.A., Mitrakas, M., Zouboulis, A.I., 2018. Application of a

1371 ceramic membrane contacting process for ozone and peroxone treatment of
1372 micropollutant contaminated surface water. J. Hazard. Mater. 358, 129–135.
1373 https://doi.org/10.1016/j.jhazmat.2018.06.060

1374 Stylianou, S.K., Kostoglou, M., Zouboulis, A.I., 2016. Ozone Mass Transfer Studies in a
1375 Hydrophobized Ceramic Membrane Contactor: Experiments and Analysis. Ind. Eng.
1376 Chem. Res. 55, 7587–7597. https://doi.org/10.1021/acs.iecr.6b01446

1377 Suez, 2007. SUEZ degremont® water handbook - Selecting ozonation reactors [WWW
1378 Document]. URL https://www.suezwaterhandbook.com/processes-and-
1379 technologies/oxidation-disinfection/oxidation-and-disinfection-using-ozone/selecting-
1380 ozonation-reactors (accessed 3.16.20).

1381 Tootchi, L., Seth, R., Tabe, S., Yang, P., 2013. Transformation products of pharmaceutically
1382 active compounds during drinking water ozonation. Water Sci. Technol. Water Supply
1383 13, 1576–1582. https://doi.org/10.2166/ws.2013.172

1384 Tu, J., Yeoh, G.H., Liu, C., 2018. Computational fluid dynamics: A practical approach,
1385 Computational Fluid Dynamics: A Practical Approach.

1386 Van Geluwe, S., Braeken, L., Van der Bruggen, B., 2011. Ozone oxidation for the alleviation
1387 of membrane fouling by natural organic matter: A review. Water Res. 45, 3551–3570.
1388 https://doi.org/10.1016/j.watres.2011.04.016

1389 von Gunten, U., 2003a. Ozonation of drinking water: Part I. Oxidation kinetics and product
1390 formation. Water Res. 37, 1443–1467. https://doi.org/10.1016/s0043-1354(02)00457-8

1391 von Gunten, U., 2003b. Ozonation of drinking water: Part II. Disinfection and by-product
1392 formation in presence of bromide, iodide or chlorine. Water Res. 37, 1469–1487.
1393 https://doi.org/10.1016/S0043-1354(02)00458-X

1394 Von Gunten, U., 2018. Oxidation Processes in Water Treatment: Are We on Track? Environ.
1395 Sci. Technol. 52, 5062–5075. https://doi.org/10.1021/acs.est.8b00586

1396 Wang, H., Zhan, J., Yao, W., Wang, B., Deng, S., Huang, J., Yu, G., Wang, Y., 2018.
1397 Comparison of pharmaceutical abatement in various water matrices by conventional
1398 ozonation, peroxone (O3/H2O2), and an electro-peroxone process. Water Res. 130, 127–
1399 138. https://doi.org/10.1016/j.watres.2017.11.054

1400 Wenten, I.G., Julian, H., Panjaitan, N.T., 2012. Ozonation through ceramic membrane
1401 contactor for iodide oxidation during iodine recovery from brine water. Desalination 306,
1402 29–34. https://doi.org/10.1016/j.desal.2012.08.032

1403 Wert, E.C., Rosario-Ortiz, F.L., Drury, D.D., Snyder, S.A., 2007. Formation of oxidation
1404 byproducts from ozonation of wastewater. Water Res. 41, 1481–1490.
1405 https://doi.org/10.1016/J.WATRES.2007.01.020

1406 Westerhoff, P., Song, R., Amy, G., Minear, R., 1997. Applications of ozone decomposition
1407 models. Ozone Sci. Eng. 19, 55–73. https://doi.org/10.1080/01919519708547318

1408 Xu, Y., Goh, K., Wang, R., Bae, T.-H., 2019. A review on polymer-based membranes for gas-
1409 liquid membrane contacting processes: Current challenges and future direction. Sep.
1410 Purif. Technol. 229, 115791. https://doi.org/10.1016/J.SEPPUR.2019.115791

1411 Yao, W., Rehman, S.W.U., Wang, H., Yang, H., Yu, G., Wang, Y., 2018. Pilot-scale
1412 evaluation of micropollutant abatements by conventional ozonation, UV/O3, and an
1413 electro-peroxone process. Water Res. 138, 106–117.
1414 https://doi.org/10.1016/J.WATRES.2018.03.044

1415 Yu, X., An, L., Yang, J., Tu, S.T., Yan, J., 2015. CO2 capture using a superhydrophobic
1416 ceramic membrane contactor. J. Memb. Sci. 496, 1–12.

https://doi.org/10.1016/j.memsci.2015.08.062

Yue, C., Seth, R., Tabe, S., Zhao, X., Hao, C., Yang, P., Schweitzer, L., Jamal, T., 2009. Evaluation of pilot-scale oxidation of several PPCPs/EDCs (pharmaceuticals and personal care products/endocrine disrupting compounds) during drinking water ozonation treatment. Water Sci. Technol. Water Supply 9, 577–582. https://doi.org/10.2166/ws.2009.573

Zhang, W., Wahlgren, M., Sivik, B., 1989. Membrane Characterization by the Contact Angle Technique II. Characterization of UF-Membranes and Comparison between the Captive Bubble and Sessile Drop as Methods to obtain Water Contact Angles. Desalination 72, 263–273. https://doi.org/10.1016/0011-9164(89)80011-6

Zhang, Z.E., Yan, Y.F., Zhang, L., Ju, S.X., 2014. Hollow fiber membrane contactor absorption of CO2 from the flue gas: review and perspective. Glob. Nest J. 16, 354–373. https://doi.org/10.1109/HICSS.2009.259

Zimmermann, S.G., Wittenwiler, M., Hollender, J., Krauss, M., Ort, C., Siegrist, H., von Gunten, U., 2011. Kinetic assessment and modeling of an ozonation step for full-scale municipal wastewater treatment: Micropollutant oxidation, by-product formation and disinfection. Water Res. 45, 605–617. https://doi.org/10.1016/j.watres.2010.07.080

Zoumpouli, G., Baker, R., Taylor, C., Chippendale, M., Smithers, C., Xian, S., Mattia, D., Chew, J., Wenk, J., 2018. A Single Tube Contactor for Testing Membrane Ozonation. https://doi.org/10.3390/w10101416